JACS Au
AN OPEN ACCESS JOURNAL OF THE AMERICAN CHEMICAL SOCIETY

pubs.acs.org/jacsau
Perspective

Redox Processes Involving Oxygen: The Surprising Influence of Redox-Inactive Lewis Acids

Davide Lionetti, Sandy Suseno, Angela A. Shiau, Graham de Ruiter, and Theodor Agapie*

Cite This: JACS Au 2024, 4, 344−368
Read Online

ABSTRACT: Metalloenzymes with heteromultimetallic active sites perform chemical reactions that control several biogeochemical cycles. Transformations catalyzed by such enzymes include dioxygen generation and reduction, dinitrogen reduction, and carbon dioxide reduction—instrumental transformations for progress in the context of artificial photosynthesis and sustainable fertilizer production. While the roles of the respective metals are of interest in all these enzymatic transformations, they share a common factor in the transfer of one or multiple redox equivalents. In light of this feature, it is surprising to find that incorporation of redox-*inactive* metals into the active site of such an enzyme is critical to its function. To illustrate, the presence of a redox-inactive Ca^{2+} center is crucial in the Oxygen Evolving Complex, and yet particularly intriguing given that the transformation catalyzed by this cluster is a redox process involving four electrons. Therefore, the effects of redox inactive metals on redox processes—electron transfer, oxygen- and hydrogen-atom transfer, and O−O bond cleavage and formation reactions—mediated by transition metals have been studied extensively. Significant effects of redox inactive metals have been observed on these redox transformations; linear free energy correlations between Lewis acidity and the redox properties of synthetic model complexes are observed for several reactions. In this Perspective, these effects and their relevance to multielectron processes will be discussed.

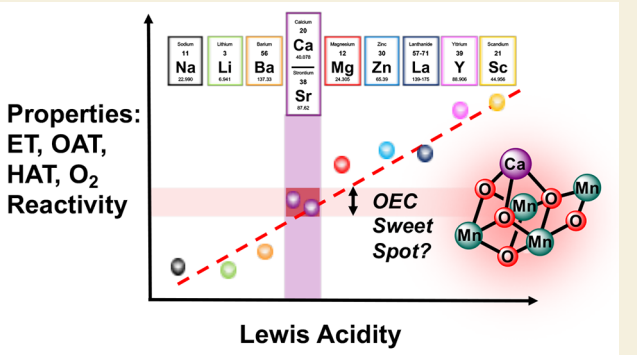

KEYWORDS: *multimetallic effects, redox reactions, metal ion-coupled electron transfer, oxygen transformations, Lewis acids, bioinorganic chemistry*

1. INTRODUCTION

The conversion of small molecules such as O_2, N_2, CO_2, H_2O, and H_2 into value-added chemicals or liquid energy carriers is important in (i) the context of solar energy conversion and storage, (ii) the efficient use of inexpensive feedstocks, and (iii) the sustainable generation of bulk chemicals. However, transforming these small molecules into useful chemicals is challenging due to the number of e^-/H^+ equivalents transferred and in terms of the necessity for controlling selectivity and the performance of the chemistry at low overpotentials.[1] The biological catalysts for small molecule conversions are proteins that often involve complex inorganic active sites: Mn_4Ca in Photosystem II (PSII) for O_2 evolution;[2] Cu_3 in laccase and CuFe in cytochrome *c* oxidase for O_2 reduction;[3] Fe_4Ni or CuMo in CO dehydrogenase (CODH) for CO_2 reduction;[4] Fe_8, Fe_7Mo, or Fe_7V in nitrogenase for N_2 reduction;[5] Fe_6 or FeNi in hydrogenase, for proton reduction and hydrogen oxidation.[6] In many of these gas-processing enzymes, two or more types of metals are found in their active sites. Accordingly, the interactions between different metal centers and their influence on structure and reactivity have been investigated in numerous synthetic systems and have also been the subject of several reviews.[7−28]

Among the enzymes that depend on heteromultimetallic active sites, two systems are unusual for the involvement of metal ions that are redox-inactive, namely (i) the oxygen evolving complex (OEC) of Photosystem II, which contains a Ca^{2+} ion and catalyzes the oxidation of H_2O to O_2, and (ii) Cu/Zn-dependent superoxide dismutase (Cu/Zn-SOD), which catalyzes the disproportionation of superoxide ($O_2^{\bullet-}$) to H_2O_2 and O_2 at an active site containing a redox-inactive Zn^{2+} ion.[2,29] Because both enzymes are involved in oxygen chemistry, their structural/activity relationships bear great relevance for energy science and industrial processes. Not

Received: October 31, 2023
Revised: December 12, 2023
Accepted: December 13, 2023
Published: January 22, 2024

https://doi.org/10.1021/jacsau.3c00675
JACS Au 2024, 4, 344−368

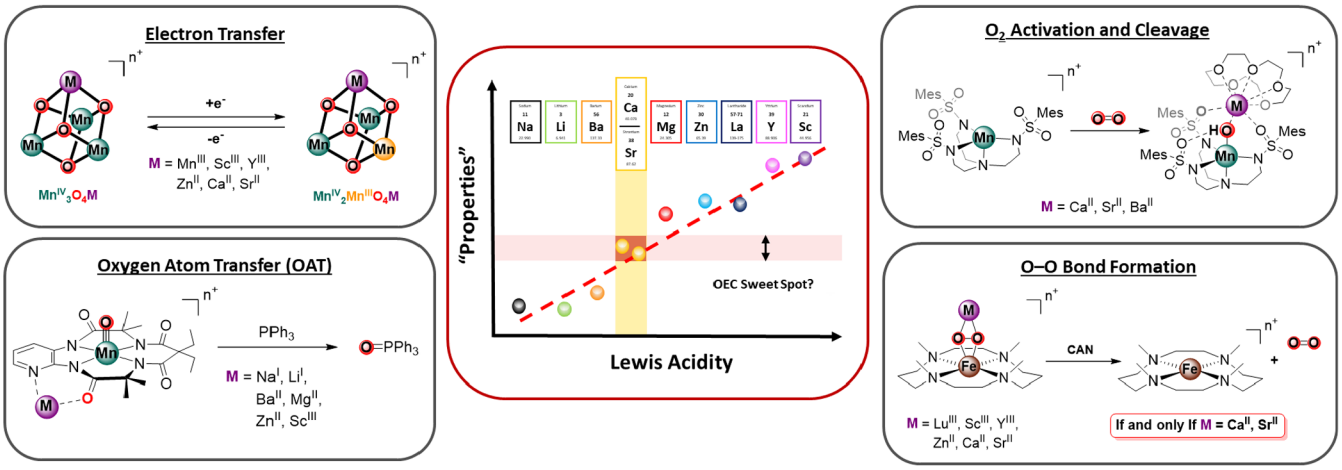

Figure 1. Lewis acid effects on redox processes involving oxygen. The linear correlation between the pK_a of the metal aqua ion and the "properties" of corresponding metal complexes (center) are universally found among many transformations that involve oxygen including (i) electron transfer (top left), (ii) oxygen-atom transfer (bottom left), (iii) O_2 activation and cleavage (top right), and (iv) O–O bond formation (bottom right).

surprisingly, many investigations have probed the role of these redox-inactive metal ions in catalysis. While a primarily structural role has been ascribed to Zn^{2+} in Cu/Zn-SOD,[3,30−32] with SOD activity being largely retained upon Zn^{2+} loss,[30] the role of Ca^{2+} in the OEC has not been conclusively elucidated. Consequently, synthetic models of the OEC have been targeted with the aim of unraveling fundamental reactivity relevant to biological water oxidation.[33−35] Interest in the effects of redox-inactive metals on redox processes involving oxygen has been further piqued by discoveries in the field of heterogeneous catalysis, where mixed-metal oxides containing both redox-active and -inactive components have gained significant attention as electrocatalysts in the oxygen evolution reaction (OER).[36−40] Moreover, employing multiple different metal centers in discrete complexes can likewise result in new physical properties and reactivity pathways beyond oxygen chemistry.[41−46] As a result, aspects of the effects of redox inactive metals on the redox reactivity of transition metals with oxygen have been addressed in several types of reactions, and this field has seen significant increase in research activity.[47−55]

Herein, we provide an overview of the literature concerning the behavior of well-defined molecular systems displaying a combination of redox-active and redox-inactive metals in the context of oxygen-related chemistry. Effects of redox-inactive metals on electron transfer (ET), oxygen-atom transfer (OAT), hydrogen-atom transfer (HAT), as well as O–O bond cleavage and formation, will be discussed (Figure 1). Because of their inability to directly participate in redox processes, the basis for controlling reactivity with redox-inactive metals must leverage properties such as their charge, size, polarizability, and/or coordination number. Given the complex interplay between these features, many (though not all) studies in this area have shown that the observed effects on redox properties cannot be ascribed to a single factor, but rather to the broader concept of Lewis acidity invoked by constructing linear free-energy relationships based on experimental properties (e.g., reduction potentials, reaction rates). Because Lewis acidity is not a well-defined quantitative parameter, several alternative scales have been developed in an attempt to provide a semiquantitative measure of Lewis acidity.[56,57] Methods based on nuclear magnetic resonance (NMR)[58,59] or fluorescence spectroscopy,[60,61] for instance, have been successfully implemented in various contexts. A scale of Lewis acidity based on electron paramagnetic resonance (EPR) measurements has also been developed by Fukuzumi and co-workers.[62] Our work has relied on the pK_a value of metal–aqua ions as a measure of Lewis acidity in part due to the availability of values for mono-, di-, and trivalent ions.[56,63−65] These values also emerge from the same interplay between distinct factors that makes use of individual parameters often inadequate to explain experimental observations. Overall, useful correlations between Lewis acidity and various types of electron- and group-transfer reactivity exist across many transition metal compounds of varying composition, nuclearity, and complexity.

In this Perspective, correlations between observed properties and Lewis acidity will be presented using the methods for quantification of Lewis acidity described in the original publications, including in cases where other parameters (e.g., ionic radius or charge) were found to provide a more satisfactory correlation. In cases where such correlations were not originally provided, or in cases where a comparison across systems originally relying on different Lewis acidity scales would be particularly insightful, the pK_a of metal–aqua ions will be used as the measure of Lewis acidity. Values for the pK_a of a broad series of metal–aqua ions are shown in Table 1. The majority of these values were obtained from the extensive lists reported by Perrin;[63] wherever possible, values extrapolated to $I = 0$ were chosen to best represent thermodynamic values. It should be noted, however, that significant variance exists for the pK_a of metal–aqua ions in different sources, especially for transition metal ions.[64,66,67] Therefore, where significantly different values ($\Delta pK_a \geq 0.5$) have been cited in other literature sources, these values were also included in the table. For the purposes of identifying correlations between observable properties (reduction potentials, reaction rates, etc.) and Lewis acidity in this Perspective, the Perrin values[63] were used (with the exception of the values for K^+, Cs^+, and Rb^+, which were recently extrapolated on the basis of ^{31}P NMR experiments).[56] Nonetheless, the uncertainties inherent in these values make quantitative interpretations of such correlations challenging, and these relationships will therefore be discussed here primarily in qualitative terms.

https://doi.org/10.1021/jacsau.3c00675
JACS Au 2024, 4, 344−368

Table 1. pK_a of $[M(H_2O)_m]^{n+}$ Species

M^{n+}	pK_a[a]	M^{n+}	pK_a[a]	M^{n+}	pK_a[a]
Mn^{3+}	0.20 (−0.6)[b]	Eu^{3+}	8.03 (8.6)[b]	Ni^{2+}	9.86
Co^{3+}	0.66 (0.5)[b] (1.75)[c]	Y^{3+}	8.04	Mn^{2+}	10.59
Fe^{3+}	2.19	Dy^{3+}	8.10	Mg^{2+}	11.40
Ga^{3+}	2.92	Tb^{3+}	8.16	Ca^{2+}	12.60
In^{3+}	3.54	Gd^{3+}	8.40 (9.78)[c]	Sr^{2+}	13.18
Al^{3+}	4.90	Nd^{3+}	8.43 (9.0)[c]	Li^{+}	13.11 (13.6)[b] (13.8)[c]
Sc^{3+}	4.93 (4.3)[b]	Co^{2+}	8.90 (9.7)[b] (9.85)[c]	Ba^{2+}	13.40
Cu^{2+}	7.34	Zn^{2+}	8.96	Na^{+}	14.80 (13.9)[b]
Lu^{3+}	7.66 (8.2)[b]	La^{3+}	9.06 (8.5)[b]	K^{+}	16.06[d] (14)
Pb^{2+}	7.78	Cd^{2+}	9.30 (10.1)[b]	Cs^{+}	16.29[d]
Yb^{3+}	8.01	Fe^{2+}	9.30 (6.8)[c]	Rb^{+}	16.34[d]

[a]pK_a values from ref 63 except where otherwise noted. [b]pK_a values from ref 67. [c]pK_a values from ref 64. [d]pK_a values from ref 56.

2. ELECTRON TRANSFER AND LEWIS ACIDS

Lewis acids have been shown to affect reduction potentials and rates of electron transfer in transition metal compounds (Figures 2 and 3). These effects were observed either upon addition of excess redox inactive metal ion to solutions of transition metal complexes displaying a basic site for binding of additional metal ions or by utilizing well-defined heterometallic complexes.

One of the more broadly studied effects of Lewis acids on electron transfer involves the conjugation of redox-active metal complexes to crown-ethers (Figure 2).[68−88] Extensive studies on mono- (**1**) and bimetallic (**2**) manganese Schiff-base complexes first appeared in the 1990s that aimed to elucidate the properties of manganese-dependent enzymes (including the OEC).[70−72] While salen-type related ligands have been shown to be useful for binding or sensing of a wide variety of redox-inactive metals via coordination to O atom donors (e.g., phenoxide),[89] inclusion of crown-ether motifs enables stronger binding of Lewis acidic ions with stoichiometric control. Exposing complex **1** to Li^+, K^+, Ca^{2+}, or Ba^{2+} leads to incorporation of a single redox-inactive metal into the crown-ether moiety, resulting in a positive shift in reduction potential for the Mn^{III}/Mn^{II} redox couple.[72] Nearly identical behavior was displayed by the μ-oxo dimer of **1**, although the observed redox couples corresponded to the two-electron reduction of the $[Mn^{III}_2O]$ core in this instance. A similar effect was observed in a related system (**7**), where the less rigid aminopropane backbone enables isolation of a bridged $(\mu\text{-}O)_2$ complex. Incorporation of redox-inactive metal ions in this $Mn^{IV}-(O)_2-Mn^{IV}$ species leads to positive shifts in potential for the $Mn^{IV}_2/Mn^{III}Mn^{IV}$ and $Mn^{III}Mn^{IV}/Mn^{III}_2$ redox couples, though only redox-inactive metals with a narrow range of Lewis acidities (ΔpK_a. = ∼2.0) were investigated.[71] A similar

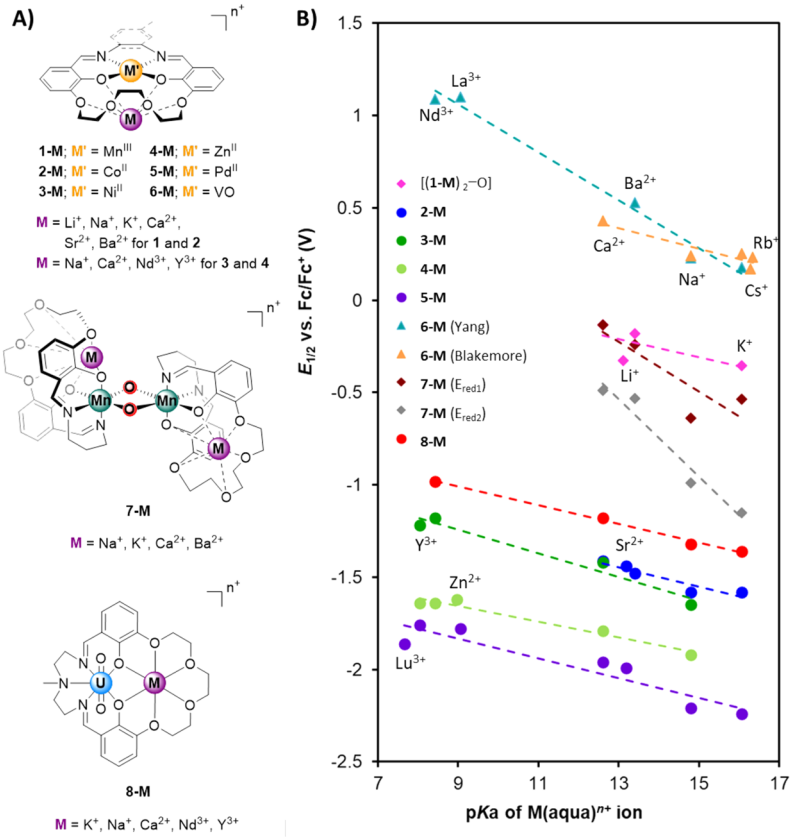

Figure 2. Linear correlation between the reduction potential of crown-ether supported (multinuclear) metal complexes and the Lewis acidity of redox-inactive metal ions. (A) Selection of crown-ether supported metal complexes. (B) Observed linear correlation is shown for complexes **1-M** (μ-oxo dimer, pink diamonds),[72] **2-M** (blue dots),[68] **3-M** (dark green dots),[78] **4-M** (light green dots),[85] **5-M** (purple dots),[84] **6-M** (salen-type backbone, teal triangles),[86] **6-M** (modified backbone, orange triangles),[87] **7-M** (two redox events, maroon and gray diamonds, respectively),[71] and **8-M** (red dots).[77]

https://doi.org/10.1021/jacsau.3c00675
JACS Au 2024, 4, 344−368

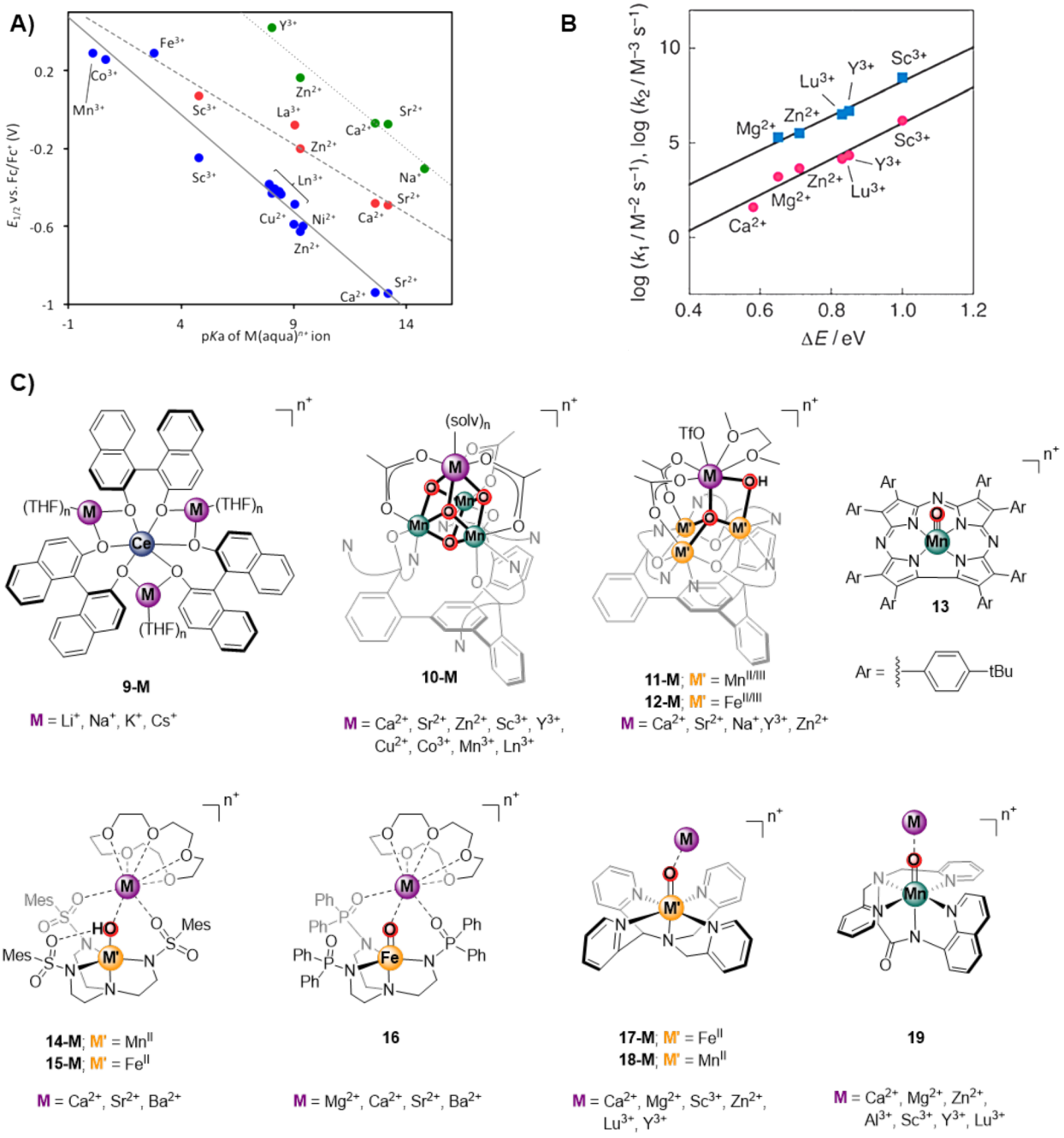

Figure 3. Linear correlation between the reduction potential of (multinuclear) metal complexes and the Lewis acidity of redox-inactive metal ions. (A) Observed linear correlation is shown for Mn_3MO_4 (**10-M**; blue), $Mn_3MO(OH)$ (**11-M**; green), and $Fe_3MO(OH)$ (**12-M**; red) type clusters; Ln = La, Nd, Eu. Gd, Tb, Dy, Yb, Y. (B) Linear correlation observed for the rate of electron transfer between **17-M** and ferrocene. (C) Selection of metal complexes that demonstrate modulation of the reduction potential upon interaction with redox-inactive metal ions. Figure 3B is reproduced from ref 149. Copyright 2011 American Chemical Society.

set of redox-inactive metals (Na^+, K^+, Ca^{2+}, Sr^{2+}, and Ba^{2+}) was screened in structurally related cobalt complexes (**2-M**). In these complexes, a linear correlation between the pK_a of the redox-inactive metal and the reduction potential of the $Co^{II/I}$ redox-couple was observed, though the narrow range of Lewis acidities once again limits generalization of this relationship.[68] Related nickel,[78] iron,[83] zinc,[85] palladium,[84] and vanadyl[86,87] complexes (**3-M** to **6-M**) have been shown to display similar correlations between the reduction potential of the complex (typically corresponding to a metal-centered ET process, though a ligand-based one for Pd and Zn) and the Lewis acidity of a wider range of cations (e.g., Na^+, Ca^{2+}, Nd^{3+}, Y^{3+}). Incorporating a more flexible triamine-based backbone enables coordination of these Schiff-base ligands to the uranyl cation ($[UO_2]^{2+}$; **8**) and thereby enables the extension of these relationships to actinide complexes. The Lewis acidity of the incorporated redox-inactive metals (K^+, Na^+, Ca^{2+}, and Nd^{3+}) linearly modulates the reduction potential of the U^{VI}/U^{V} redox couple. Notably, the reversibility of the observed electrochemical processes is also affected by the Lewis acidity of the

https://doi.org/10.1021/jacsau.3c00675
JACS Au 2024, 4, 344−368

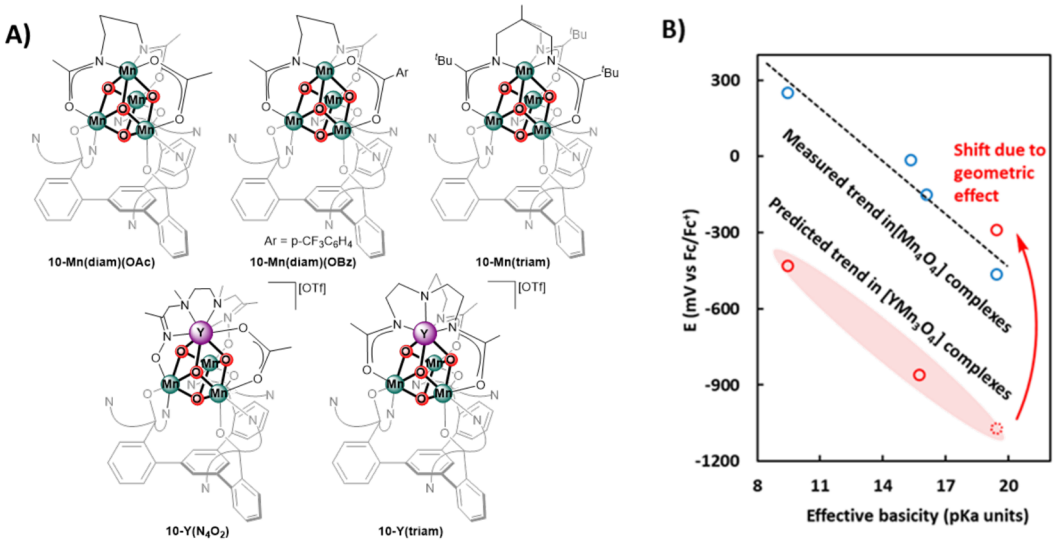

Figure 4. Plot of reduction potential vs effective basicity for a series of cubane complexes. (A) Selection of metal-oxo clusters. (B) Linear correlation between reduction potential and effective ligand basicity in $[Mn_4O_4]$ complexes, including **10-Mn** (blue circles). Similar trend expected in $[YMn_3O_4]$ complexes, including **10-Y** (red circles), with the exception of trisamidate complex **10-Y(triam)** due to geometric effects. Graph adapted from ref 119. Copyright 2019 American Chemical Society.

redox-inactive metal ions, with evidence of downstream chemical reactivity for more Lewis acidic divalent and trivalent redox-inactive cations.[77]

Heterobimetallic complexes with other ligands containing phenolate moieties have also been reported, although they frequently involve a combination of two redox-active metals.[90−103] In these complexes, some effects can be attributed to the Lewis acidity of a metal ion, but their properties are mainly dominated by electrostatic effects. Notable exceptions are the rare-earth/alkali-metal heterobimetallic complexes (**9**) reported by Walsh and Schelter.[104−106] Binding of redox-inactive metals to cerium complexes supported by binolate ligands modulates the reduction potential for the $Ce^{IV/III}$ couple. Different redox-inactive metals were also found to promote formation of chemical oxidation products featuring diverse binding modes of the Lewis acidic ions as a function of their identity.

Our group has extensively studied the effects of Lewis acidity on reduction potentials in multimetallic cluster complexes (**10-M** to **12-M**).[67,107−111] Some of these clusters (**10-M**) closely match the structural aspects of the OEC, for which only a few well-defined structural examples have been reported.[112−116] These tetraoxido clusters display a $[Mn_3CaO_4]$ "cubane" structural motif, with the redox-inactive metal situated at the apical position (**10-M**; Figure 3).[108,109] In these compounds, the potential for the $Mn^{IV}{}_3/Mn^{III}Mn^{IV}{}_2$ redox couple shifts from −0.94 V (vs the ferrocenium/ferrocene couple, hereafter denoted $Fc^{+/0}$) for Sr^{2+} to +0.29 V for Mn^{3+}, and correlates linearly with the Lewis acidity of the corresponding metal ion. The linear fit is observed over a wide pK_a range ($\Delta pK_a \sim 15$), which allows a broader demonstration of the trend, and displays a potential shift of *ca.* 0.1 V for every pK_a unit (Figure 3A; blue dots). Rather than Lewis acidity, computational studies of the OEC incorporating different redox-inactive cations suggested a correlation between the reduction potentials of the clusters and the charge of these redox-inactive cations.[67] Notably, the protein environment that encages the OEC cluster in Photosystem II imposes bonding pressures from all directions.[117,118] This is in contrast with synthetic cubane compounds, where the carboxylate bridges do not place a similar constraint on the apical, redox-inactive metal center. To address the potential effects of geometric constraints of the protein environment on the OEC cluster, synthetic cubane variants with chelating amidate ligands were prepared (Figure 4). Interestingly, a caveat to the correlation between the reduction potential and the Lewis acidity trend was observed in these systems. In a series of $[Mn_4O_4]$ (**10-Mn**) and $[YMn_3O_4]$ (**10-Y**) cubane clusters,[119] our group showed that ligand basicity modulates the reduction potentials of the clusters in a similar fashion to reported $[Co_4O_4]$ and $[RuCo_3O_5]$ complexes.[120,121] However, the tris-amidate substituted YMn_3O_4 (**10-Y(triam)**) cluster displays a 140 mV positive shift in the potential for the $[YMn^{IV}{}_3]/[YMn^{IV}{}_2Mn^{III}]$ couple relative to the tris-acetate cluster (**10-Y**), inconsistent with the increased basicity of amidates versus acetates. This exception can be explained by geometric changes in the cluster core due to ligand steric constraints—chelating tris-amidate ligands contract the Y−oxo distances by roughly 0.1 Å compared to the those in the tris-acetate cluster, decreasing the electron density available at the Mn centers. Relevant to the cation size dependence on the activity of the OEC, these results suggest geometric constraints may cause nonlinear changes in reduction potentials and reactivity, engendering more pronounced effects than those predicted on the basis of its lower Lewis acidity. In other words, a larger metal may behave like a smaller, more Lewis acidic one of the same charge, resulting in a correlation of properties with charge, not Lewis acidity.

The role of the number of μ-oxo ligands was also investigated with similar tetranuclear complexes **11-M** and **12-M**,[107,110] which feature a $[M_3(\mu_4\text{-O})(\mu_2\text{-OH})M']$ core (M = Mn, Fe; M' = redox-inactive metal; Figure 3). The Lewis acidity of the redox-inactive metal influences the potential for the $M^{III}{}_3/M^{III}{}_2M^{II}$ couples, which shift from $E_{1/2}$ = −0.30 to +0.42 V (vs $Fc^{+/0}$) for M = Mn (Figure 3A, green dots) and −0.49 to +0.07 V for M = Fe (Figure 3A, red dots) as the Lewis acidity of the incorporated redox-inactive metal increases.

https://doi.org/10.1021/jacsau.3c00675
JACS Au 2024, 4, 344−368

Based on the observations from the two series of [Mn_3] complexes, it appears that reducing the oxo content results in a positive shift (~0.5 V) in the reduction potential of the corresponding cluster. Despite the higher Mn oxidation states in cubane-type vs oxo-hydroxo complexes ([Mn^{IV}_3] vs [Mn^{III}_3] in the oxidized forms, respectively), the presence of additional electron-rich O^{2-} moieties increases the electron density around the metal centers, shifting the cluster's reduction potential to more negative values compared to complexes **11-M** and **12-M**. Intriguingly, the nearly identical reduction potentials engendered by calcium and strontium in each series support the hypothesis that redox-inactive metals might be involved in the tuning of reduction potentials in PSII, as substitution of Ca^{2+} with Sr^{2+} uniquely enables retention of catalytic competence in this system. It must be noted, however, that in computational studies of the OEC, substituting Ca^{2+} for other redox-inactive metals did not produce a linear correlation between the redox properties of the OEC and the Lewis acidity of the redox-inactive metals.[67]

The effects of calcium and strontium on electrochemical properties have also been studied in a series of Fe (**14**) and Mn (**15**) complexes supported by tripodal tris(sulfonamido) (MST) ligands.[122,123] Remarkable rate enhancements in O_2 activation by Fe^{II}/Mn^{II} precursors were observed upon addition of Ca^{2+} and Sr^{2+} to generate Fe^{III}/Mn^{III}−(OH)−M complexes **14-M** and **15-M**, whereas only limited effects were observed upon the addition of less Lewis acidic Ba^{2+}. The reduction potentials of complexes **14-Ba** and **15-Ba** were also found to be significantly more negative (by ~0.06−0.10 V) than those of the isostructural Ca^{2+} and Sr^{2+} analogues. The observation of only minor differences in reduction potential between Ca^{2+} and Sr^{2+} complexes (e.g., ~0.02 V for **15-Ca** vs **15-Sr**) led the authors to assert that Lewis acidity alone is not sufficient to explain the observed trends, since a larger difference might be expected for Ca^{2+} vs Sr^{2+}. Nonetheless, the difference in Lewis acidity between these congeners is indeed small ($\Delta pK_a < 1$); accordingly, very similar reduction potentials may be expected for Ca and Sr complexes (*vide supra*).[107,108,110] A related trisphosphinamide ligand framework, also developed by the Borovik group, was shown to enable anchoring of a variety of 18-crown-6 encapsulated Lewis acids in the proximity of a terminal iron−oxo motif (**16**).[124] Although no electrochemical data were reported for this series, the linear trend between pK_a and the energy of the first electronic absorption band was described, indicating that binding of the Lewis acid modulates the molecular orbital energies of the Fe complexes.

Another important class of compounds that display similar effects on ET are complexes that bear high-valent terminal metal−oxo moieties. In nature, these metal−oxo motifs are ubiquitous as intermediates in many oxidative transformations,[16,125−131] and have even been suggested in biological water oxidation.[2,132] Consequently, intensive efforts have been undertaken to study these motifs in synthetic model complexes.[127,133−145] The well-defined nature of many of these systems has also enabled systematic investigations into the effects of Lewis acids on their properties and reactivity. Although many of these complexes are also competent for OAT, HAT, O_2 activation, and/or O−O bond cleavage, their reactivity in these types of transformations will be discussed in later sections (*vide infra*), and the current discussion will remain focused on electron-transfer reactions.[146−154]

One of the first studies of the effect of redox-inactive metals on high-valent terminal Fe^{IV}−O complexes was reported with a cyclam macrocycle.[154,155] $(TMC)Fe^{IV}(O)^{2+}$ (**27**; TMC = *N*,*N*′,*N*″,*N*‴-tetramethylcyclam) behaves as a one electron oxidant toward excess ferrocene;[156] however, addition of Sc^{3+} induces a change in the redox chemistry of $(TMC)Fe^{IV}(O)^{2+}$ and a second electron transfer to complex **27** from Fc is observed.[154] Kinetic studies confirmed that the reaction proceeds via a rate-determining 1e$^-$ reduction, followed by a fast second ET step. Interestingly, Ca^{2+} induces a similar shift in the reactivity of complex **27**, albeit only when present in large excess (40 equiv vs 2 equiv for Sc^{3+}).[154] These observations are consistent with a more positive reduction potential of the Fe^{IV}=O complex upon binding of Lewis acids. Direct evidence for binding of Sc^{3+} to terminal iron-oxo moiety was provided by X-ray diffraction studies on an isolated complex assigned as $[(TMC)Fe^{IV}(O)-Sc(OTf)_4(OH)]$. Recent reports based on computational modeling and Mössbauer and EPR data, however, have cast doubt on this assignment, suggesting the complex $[(TMC)Fe^{III}-(OH)-Sc(OTf)_4(H_2O)]$ as the most likely identity of the species characterized by crystallography.[157,158]

Peroxide complexes of the form $[(TMC)Fe^{III}(O_2^{2-})M]^{n+}$ (**26-M**, M = Ca^{2+}, Sr^{2+}, Zn^{2+}, Lu^{3+}, Y^{3+}, Sc^{3+}) can be generated from the same Fe^{II} precursor used in preparation of **27** (a process which is itself dependent on the identity of the redox-inactive metal, see Section 4). Electrochemical investigations indicated that the irreversible 1e$^-$ reduction potentials correlate linearly with the Lewis acidity of the redox-inactive metal ions. Additionally, the rate for ET between complexes **26-M** and 1e$^-$ reductants (e.g., bromoferrocene) is also dependent on Lewis acidity, with a plot of log(k) vs Lewis acidity displaying a linear correlation (Figure 6B, blue dots). In the same series, the lower Lewis acidity of Ca^{2+} and Sr^{2+} additionally engendered a shift in the potential required for the oxidation of the complex to values sufficiently negative to enable chemical oxidation resulting in O_2 evolution (see Section 5 for details on this reactivity), while complexes containing stronger Lewis acids did not show evidence for electrochemical oxidation. Notably, peroxo complex **26** can itself be oxidized (both electrochemically and with chemical oxidants) to generate **25** and O_2; therefore, the unique behavior of the Ca^{2+} and Sr^{2+} complexes is most accurately ascribed to these ions being the only ones in this series whose Lewis acidity is sufficiently low for the relevant oxidation to occur at moderate potential, while stronger Lewis acids shift the potential for this oxidation too far positively for analogous behavior to be observed.

Complex $[(N4Py)Fe^{IV}(O)]^{2+}$ (**17**; Figure 3C)), supported by a tetrapyridine ligand, also exhibited intriguing behavior in the presence of Lewis acidic metal ions.[149] The redox properties of this complex were shown to be affected by Sc^{3+} ions, enabling the oxidation of $[Fe^{II}(bpy)_3]^{2+}$, whose potential ($E_{1/2}$ = +1.06 vs SCE) is normally too positive to allow oxidation by **17** (E_{red} = +0.51).[156] Additional experiments suggested that the reduction potential for **17-Sc** ranges between +1.26 and +1.35 V (vs SCE), an increase of ~0.8 V compared to $[(N4Py)Fe^{IV}(O)]^{2+}$. Investigation of the effects of Sc^{3+} concentration on ET suggested that two Sc^{3+} ions bind to the Fe^{IV}−oxo moiety at high Sc^{3+} concentrations. Rate acceleration for ET is also observed in the presence of Sc^{3+} and other redox-inactive metal ions (Y^{3+}, Lu^{3+}, Zn^{2+}, Mg^{2+}, and Ca^{2+}), and ET rates correlate linearly with Lewis acidity

https://doi.org/10.1021/jacsau.3c00675
JACS Au 2024, 4, 344−368

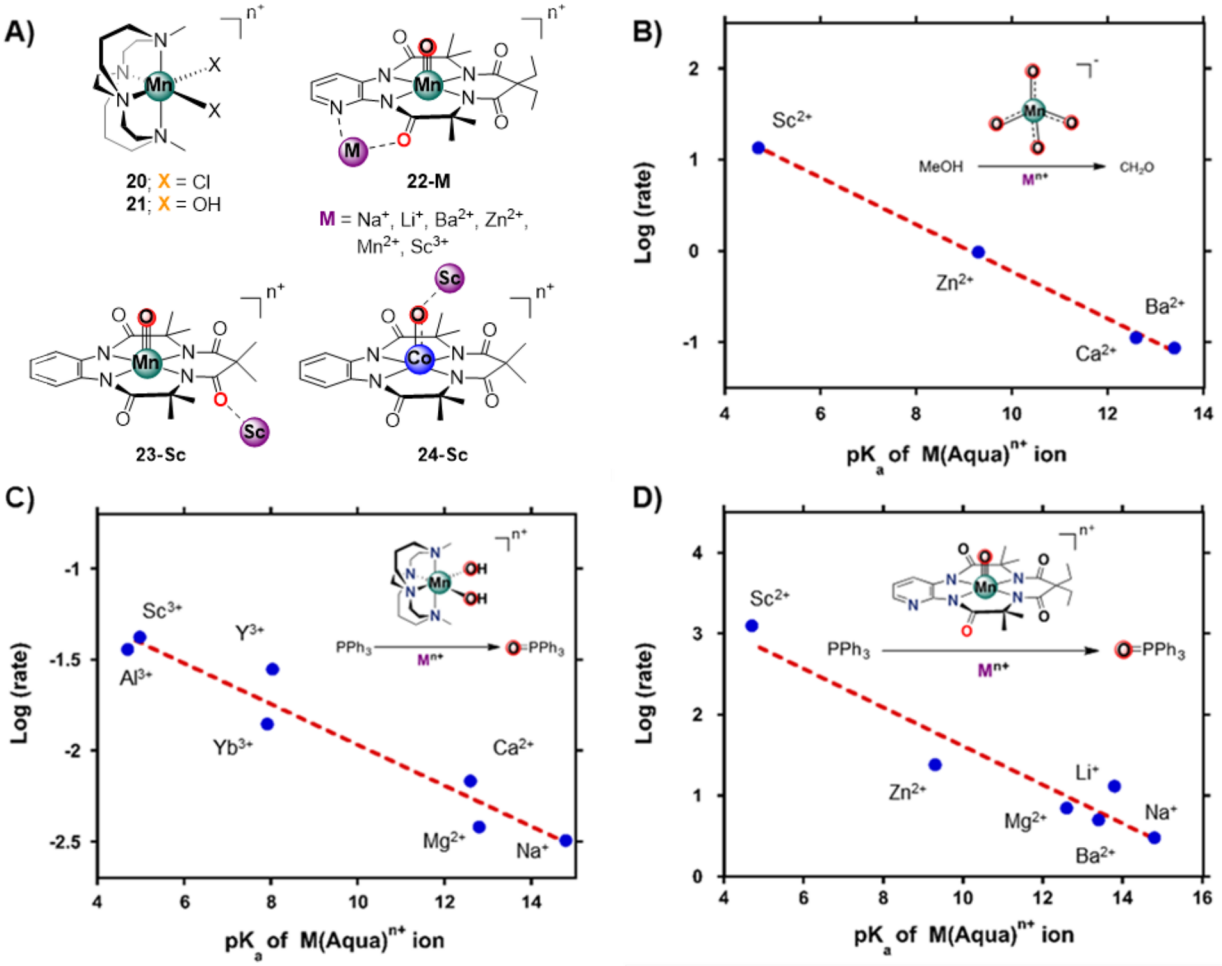

Figure 5. Linear correlation between Lewis acidity of redox-inactive metal ions and oxygen atom transfer (OAT) reactions. (A) Selection of metal complexes where the rate of oxygen atom transfer (OAT) is regulated by the Lewis acidity of bound redox-inactive metals. (B-D) Observed linear correlation between the rate of OAT and Lewis acidity of the redox-inactive metal for oxidation of methanol by permanganate (B), and oxidation of triphenylphosphine to triphenylphosphine oxide by **21** (C) and **22** (D). Figure 5B–D was generated by analyzing the data reported in refs 173, 180, and 194.

(Figure 3B). In the isostructural Mn complex $[(N4Py)\text{-}Mn^{IV}(O)]^{2+}$ (**18**) the reduction potential shifts from +0.80 V, to +1.31 V, and finally to +1.42 V (vs SCE) upon binding one and two Sc^{3+} ions, respectively.[146,152] The effect of other Lewis acidic redox-inactive metals, however, has not been reported. Similarly, $[(dpaq)Mn^{IV}(O)]^{+}\text{-}M^{n+}$ (M^{n+} = Ca^{2+}, Mg^{2+}, Zn^{2+}, Lu^{3+}, Y^{3+}, Al^{3+}, and Sc^{3+}) complexes (dpaq = 2-[bis(pyridin-2-ylmethyl)]amino-N-quinolin-8-yl-acetamidate) (**19**) showed a linear dependence between ET rate constant and Lewis acidity of M^{n+}, with increasing Lewis acidity enhancing reactivity.[159]

In studies on a related Cr complex containing a superoxide fragment, $[Cl(TMC)Cr^{III}(O_2^{\bullet-})]^{+}$, ET from $1e^{-}$ reductants to Cr was enabled by the presence of redox-inactive metals (Ca^{2+}, Mg^{2+}, Y^{3+}, Al^{3+}, Sc^{3+}), akin to the behavior exhibited by complex **17**.[160] Furthermore, consistent with the results for complex **17**, a linear correlation was observed between the logarithm of the rate of electron transfer and the Lewis acidity of the redox-inactive metal, highlighting the generalizability of these effects in complexes containing high-valent metal centers bound to oxygen-derived ligands.

Lewis acid binding was also found to tune the reduction potential of a corrolazine-supported Mn–oxo species studied by Goldberg and co-workers.[150] Using the octakis(*p-tert*-butylphenyl)corrolazinato $(TBP_8Cz)^{3-}$ ligand, a Mn^{V}–oxo complex (**13**; Figure 3C), a diamagnetic species that is unreactive towards reduction by ferrocene, was isolated. Addition of one equivalent of $Zn(OTf)_2$ results in conversion to a paramagnetic species whose spectroscopic features are consistent with formation of a corrolazine π-cation radical. Due to Zn^{2+} being redox-inactive, oxidation of the corrolazine ring indicates concurrent reduction of the Mn^{V} center via intramolecular electron transfer. The resulting species was therefore assigned as the valence tautomer complex $[(TBP_8Cz^{\bullet+})Mn^{IV}(O)\text{–}Zn^{2+}]$ (**13-Zn**). Treatment of **13-Zn** with 1,10-phenanthroline sequesters the Zn^{2+} cation and regenerates **13**, confirming the association of Zn^{2+} to the metal complex and the chemical reversibility of the intramolecular ET event. No dependence on Zn^{2+} concentration (beyond 1 equiv) was observed, suggesting that a single zinc ion is bound to the Mn complex. **13-Zn** is reduced by ferrocene or 2,4-di-*tert*-butylphenol, yielding a Mn^{IV} complex with a closed-shell corrolazine ring. This contrasts the electrochemical behavior of precursor **13** and aforementioned **27-Sc**, which are $2e^{-}$ oxidants.[154] Moreover, **13-Zn** is unique in its ability to form a 1:1 adduct with Zn exclusively, whereas other analogous

https://doi.org/10.1021/jacsau.3c00675
JACS Au 2024, 4, 344–368

Mn^{IV}−O complexes appear to be able to bind multiple redox-inactive metals.[146,152]

Valence tautomerism was also suggested during the formation of a metastable Co^{IV}−oxo complex (**24**) generated by addition of PhIO to $[(TAML)Co^{III}]^{1-}$ (TAML = tetraamido macrocyclic ligand) (Figure 5).[151] The presence of Lewis acids (e.g., Sc^{3+}, Y^{3+}, and Zn^{2+}) stabilizes complex **24**, which was predicted to be otherwise highly reactive due to population of the metal−oxo π^* orbitals. The presence of a Co^{IV}−oxo was established by extended X-ray absorption spectroscopy (EXAFS), which indicated a Co−O distance of 1.67 Å − slightly shorter compared to other reported Co^{IV}-oxo moieties.[148,161] DFT calculations carried out on complex **24** predict a doublet ground state with significant spin density on the oxygen atom, giving rise to a radical "oxyl"-type moiety and, consequently, a formal assignment of **24** as $[(TAML)Co^{III}(O^{\bullet})]^{2-}$. However, in the presence of scandium ions, the unpaired-electron spin is mainly located on cobalt, suggesting transfer of one electron from Co^{III} to oxygen leading to a $[(TAML)Co^{IV}(O)Sc]^{+}$ assignment, highlighting the role of Sc^{3+} in valence tautomerism. Earlier studies also reported on the stabilizing effect of scandium ions on high-valent Co^{IV}−oxo moieties, allowing the observation of the scandium adduct in $[(TMG_3tren)Co^{IV}(O)Sc(OTf)_3]^{2+}$ (TMG_3tren = tris[2-*N*-tetramethylguanidyl)ethyl]amine).[148] However, subsequent investigations on this system have suggested that a $[(TMG_3tren)Co^{III}(OH)Sc(OTf)_3]^{2+}$ assignment might be more accurate,[160,162] highlighting the challenges in accurately determining the oxidation state of transition metals and protonation state of bridging oxo ligands.

Taken together, these reports provide a clear insight into how redox-inactive metal ions influence the reduction potential and the rate of ET of a broad spectrum of mono- and multimetallic transition metal complexes. In most cases, experimentally determined values (e.g., reduction potential) display linear correlations with Lewis acidity, enabling extrapolation of these relationships and prediction of the properties of hitherto unexplored compounds. These effects have also been successfully modeled, in cases where binding of the redox-inactive ions is an equilibrium process, on the basis of the Nernst equation, which can be used to quantify the shift in reduction potential as a function of the differential binding of these ions to the oxidized and reduced forms of the redox-active fragment. This model, originally developed to analyze the shift in reduction potentials engendered by redox-inactive metal ions in organic fragments (e.g., flavins, quinones, and other carbonyl compounds),[50,163,164] has been successfully applied to several of the transition metal systems described in this section, especially in the context of high-valent metal−oxo complexes **17**, **18**, and **19**.[146,149,159,165] Additionally, the Marcus equation of outer-sphere electron transfer has been applied to the analysis of reactions between high-valent metal−oxo compounds and substituted ferrocenes as $1e^-$ donors in order to outline the dependence of ET rate on the driving force for electron transfer.[149]

Alternative models have been proposed to rationalize the effects of redox-inactive metal ions on the potential of transition metal complexes to those, discussed in this section, leveraging Lewis acidity to outline correlations with experimental reduction potentials and ET rates. In particular, the effects of redox-inactive metals on the potential of Co, Ni, and Fe complexes supported by salen-type ligands with appended crown ether motifs (such as those shown in Figure 2) have been ascribed to electrostatic effects engendered by the redox-inactive ions.[81,83,103,166] According to this model, the electric field generated by the Lewis acidic ions, which depends on the ionic charge and on the distance between redox-active and -inactive sites, is the primary source of shifts in reduction potential in systems in which the incorporation of redox-inactive ions does not significantly alter the ligand field at the redox-active metal center; in these cases, the redox-inactive ions can be modeled as point-charges, though quantitative analyses are complicated by the necessary estimation of dielectric constants for calculations using Coulomb's law[103] or the need for significant computational work.[166] On the other hand, in cases where Lewis acid binding perturbs the ligand field at the transition metal site more significantly (e.g., when the geometry of bridging ligands is more substantially affected by ion incorporation), both electrostatic and inductive effects are operative and must be considered for adequate analysis. It should be noted that the electrostatic model has been applied primarily in systems where only narrow ranges of redox-inactive ions were investigated (e.g., K^+, Na^+, and Ba^{2+}, $\Delta pK_a \sim 2.6$); therefore, broader series likely need to be determine to fully explore the true scope of these effects.

One common feature of the systems described in this section (and in this Perspective overall) is the absence of significant metal−metal interactions between redox-active and -inactive centers. In complexes where such metal−metal bonding interactions are present, deviations can occur as a result of the orbital overlap between adjacent metal centers.[167] In a representative example, Lu and co-workers found that the reduction potential of a series of nickel−M complexes (M = Al^{3+}, Ga^{3+}, In^{3+}) supported by tripodal ligands featuring N and P donors varies as a function of heterometal identity. However, a stronger correlation between reduction potential and the size or charge density of the redox-inactive ions, rather than their metal−aqua pK_a or other parameters was observed.[168] These findings were ascribed to the larger redox-inactive metals displaying increased overlap with the Ni^0 orbitals, resulting in a stronger effect despite the lower Lewis acidity. As metal−metal bonding involves a more direct interaction between redox-inactive and -active metals, it is perhaps unsurprising that in this and analogous cases a stronger correlation of experimental properties with parameters other than Lewis acidity (metal size, charge, or other factor) could be observed. Since metal−metal interactions have not been identified in the OEC, synthetic systems leveraging metal−metal bonds will not be discussed further in this Perspective.

3. LEWIS ACID EFFECTS ON OXYGEN ATOM TRANSFER

As evident from the previous examples, redox modulation by Lewis acids is important for various processes involving electron transfer. Lewis acid effects are also observed in the O atom transfer reactivity of high-valent metal−oxo species. In fact, some of the earliest reports of the effects of redox-inactive metals on redox processes focused on high-valent transition metal−oxo species and their reactions with various substrates in the presence of redox-inactive metals. Ruthenate ($[Ru^{V}O_2(OH)_3]^{2-}$),[169] chromate ($[Cr^{VI}_2O_7]^{2-}$),[170] permanganate ($[Mn^{VII}O_4]^{-}$),[170−173] ferrate ($[Fe^{VI}O_4]^{2-}$),[174] and nitridoosmate ($[Os^{VIII}O_3(N)]^{-}$)[175,176] were shown to be more effective oxidants in the presence of a variety of Lewis acids, including several Group 1 and 2 metals. In their seminal work, Lau and co-workers reported enhanced oxidation of the

https://doi.org/10.1021/jacsau.3c00675
JACS Au 2024, 4, 344−368

unactivated C−H bonds in cyclohexane under mild conditions by ruthenate, perruthenate, chromate, permanganate, and ferrate.[169,170,174] Formation of cyclohexanone is accelerated by addition of Zn^{2+}, Al^{3+}, Fe^{3+}, Cu^{2+}, Mg^{2+}, and Li^{+} salts, an effect that is also mildly anion-dependent. Even at this early stage, rate acceleration was proposed to involve a shift in the reduction potential due to binding of a Lewis acid to the M−O moieties of the oxoacid. Electrostatic effects were ruled out based on the observation that trifluoroborane—a *coordinating* but neutral Lewis acid—leads to rate acceleration while the positively charged, *noncoordinating* tetraphenylphosphonium cation has no effect on the reaction rates.[177] Reaction of $KMnO_4$ with methanol was also observed to be greatly accelerated (up to 10^7-fold) in the presence of Lewis acids (e.g., Ba^{2+}, Ca^{2+}, Zn^{2+}, Sc^{3+}, or BF_3).[173] Our analysis of the reported kinetic data reveals a clear linear correlation between reaction rate and the Lewis acidity of the redox-inactive metal (Figure 5B). Recently, Lau and co-workers further demonstrated cooperative effects of mildly Lewis acidic Ca^{2+} and acetic acid, a weak Brønsted acid, in activating RuO_4^- and MnO_4^- toward alkane oxidation.[178,179]

Cross-bridged cyclam-supported manganese complexes $(Me_2EBC)Mn^{II}Cl_2$ (**20**; Me_2EBC = 1,1-dimethyl-1,4,8,11-tetraazabicyclo[6.6.2]-hexadecane) and (Me_2EBC)-$Mn^{IV}(OH)_2(PF_6)_2$ (**21**) display another example of reactivity modulation by Lewis acidic ions.[180] Complex **20** is a sluggish catalyst for oxygen atom transfer to thioanisole. However, addition of redox-inactive metal salts (Na^+, Mg^{2+}, Ca^{2+}, Al^{3+}, Sc^{3+}, Y^{3+}, and Yb^{3+}) leads to more efficient catalysis, displaying accelerated oxygenation rates and an overall increase in conversion and yield.[180] Stoichiometric studies with **21** and Al^{3+} likewise showed a moderate increase in activity. Mechanistic studies suggested initial formation of an S-centered radical via metal-coupled electron transfer (MCET), a well-established mechanism for high-valent terminal metal−oxo species involving Fe and Mn (*vide infra*).[164] In the same report,[180] the stoichiometric oxygenation of triphenylphosphine by **21** afforded a direct comparison of the rate of oxygenation across a diverse series of Lewis acidic metals. A plot of log(rate) vs the pK_a of the metal-aqua species based on the reported data displays a clear linear correlation (Figure 5C).[180] In subsequent studies by the same authors, the activity of high-valent Mn−oxo species toward the epoxidation of cyclooctane was enhanced with the increasing Lewis acidity of redox-inactive metal additives.[181−183] A graphical analysis, however, could not be performed since quantitative rate data were not reported. In this system, the catalytically competent species is presumed to contain a $[Mn]-O-LA^{n+}$ moiety (LA = Lewis acid) in analogy to other published systems. However, the exact binding mode of the Lewis acid in these complexes has not been corroborated experimentally.

The presence of Lewis acids was also found to affect the O atom transfer reaction from **17** to sulfides. The rate of oxidation of thioanisoles by **17** is greatly accelerated (>10^2-fold) by Sc^{3+}.[184,185] In fact, the mechanism of oxidation was found to shift from direct O atom transfer in the absence of Sc^{3+} (a $2e^-$ step), to MCET followed by fast O atom transfer (two 1 e^- processes) in the presence of Sc^{3+}. This effect was ascribed to the increased driving force for electron transfer resulting from the positive shift in reduction potential of the Fe complex upon binding of Sc^{3+}. When this driving force is lowered, e.g., in reactions with more electron-poor thioanisoles, the extent of rate acceleration by Sc^{3+} is diminished.[185] ET to the Fe complex was found to be the rate-limiting step in the sulfide oxidation reaction,[184] which is in contrast with the mechanism of sulfide oxidation via proton-coupled electron transfer (PCET) reactions, where protonation of the metal-oxo complex was found to be rate-determining.[184,186] Oxidation of thioanisole with the analogous Mn complex **18** was also reported; binding of Sc^{3+} to **18** resulted in a marked increase in the rate of the reaction (~2200 fold), consistent with a change from direct OAT to a mechanism that involves electron transfer followed by transfer of the oxygen atom (MCET-OT).[165]

Oxygen atom transfer to PPh_3 was reported with Mn-corrolazinato complex **13**.[187] This reaction is influenced both by coordination of axial donors to the manganese metal center[188] and by tautomerization of **13** to the radical cation $[(TBP_8Cz^{\bullet+})Mn^{V}(O)]$.[189] As discussed above, addition of Zn^{2+} induces valence tautomerism to the corresponding complex **13-Zn** (Figure 3C).[150] While in the thus far described examples, Lewis acid binding resulted in an *increase* in OAT, somewhat surprisingly, here a decrease (>10^3) in the rate of OAT from **13** to PPh_3 is observed upon binding of Zn^{2+} or other Lewis acids (i.e., H^+ and $B(C_6F_5)_3$).[190] Mechanistic studies indicated that OAT from $[(TBP_8Cz^{\bullet+})Mn^{IV}(O)$-$Zn^{2+}]$ to PPh_3 proceeds via the same pathway as for $[(TBP_8Cz)$-$Mn^{V}(O)]$, involving direct nucleophilic attack of PPh_3 on the electrophilic Mn−oxo moiety. Additional investigations also revealed that oxygen atom transfer is influenced by the steric environment of the corrazoline ligand and substitution pattern of the triphenylphosphine. Electrochemical experiments indicated that the reduction potential of **13** shifts positively by ~0.70 V upon binding of Zn^{2+}. Nonetheless, the reduction potentials of −0.05 V and +0.69 V (vs SCE) for **13** and **13-Zn**, respectively, are not sufficiently positive to enable one-electron transfer from PPh_3 (E_{ox} = +2.97 V vs SCE),[190,191] ruling out a shift to an ET-OT mechanism as observed in the case of the stronger $1e^-$ oxidants **17** and **18**. It is speculated that that the two-electron electrophilicity for $[(TBP_8Cz^{\bullet+})Mn^{IV}(O)$-$Zn^{2+}]$ is reduced by Zn^{2+} binding (potentially due to steric effects), resulting in a slower concerted OAT.[190] DFT calculations and experimental studies furthermore suggest that the spin state of the Mn−oxo moiety, which is known to influence reactivity,[192,193] might also be responsible for the observed behavior in this system.[193]

An alternative approach to binding of redox-inactive ions to metal−oxo motifs under dynamic equilibrium binding conditions is to provide a dedicated binding site for redox-inactive metal ions on the same multidentate ligand scaffold.[194] This approach has been successfully employed in complexes bearing high-valent Mn^{V}−oxo moieties that are supported by tetraanionic macrocyclic ligands (TAML; **22-M**; Figure 5A). Generally, Mn^{V}−oxo species supported by TAML ligands display diminished reactivity due to the stabilization of the high-valent Mn center by the electron-rich framework.[195] The presence of a pyridine donor in the TAML ligand in **22**, however, allows binding of a wide variety of redox-inactive metal ions (Na^+, Li^+, Ba^{2+}, Zn^{2+}, Mg^{2+}, and Sc^{3+}) to a secondary site, which drastically affects its reactivity in oxygen atom transfer.[194] Binding of Lewis acids to the backbone pyridine site, confirmed via infrared (IR) spectroscopy, accelerates the rate of PPh_3 oxygenation upon addition of the above-mentioned redox-inactive metals, and our analysis showed that the log(rate) of PPh_3 oxidation correlates linearly with the Lewis acidity of the respective ions (Figure 5D).

https://doi.org/10.1021/jacsau.3c00675
JACS Au 2024, 4, 344−368

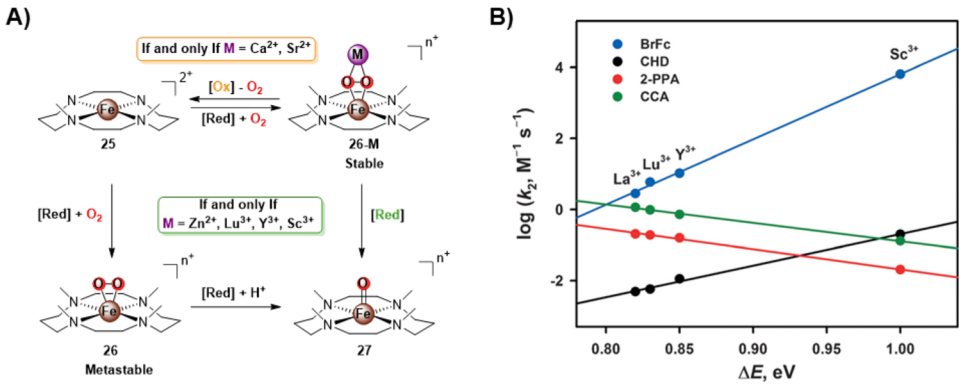

Figure 6. Activation of [(TMC)Fe^{II}] by dioxygen and the linear correlation between the Lewis acidity of redox-inactive metal ions and reactivity from the resulting iron-peroxo species [(TMC)$Fe^{II}(O_2)$]. (A) Reactivity of [(TMC)Fe^{II}] (**25**) in the presence of redox-inactive metals and dioxygen and subsequent transformations upon oxidation and/or reduction of the resulting iron-peroxo species. (B) Linear correlation between the Lewis acidity of redox-inactive metals in **26-M** (M = Ca^{2+}, Sr^{2+}, Zn^{2+}, Lu^{3+}, Y^{3+}, and Sc^{3+}) and the rate of (i) electron transfer with bromoferrocene (blue dots/traces), (ii) hydrogen atom abstraction from cyclohexadiene (black dots/traces), and (iii and iv) deformylation of 2-phenylpropionaldehyde (red dots/traces) or cyclohexane carboxaldehyde (green dots/traces). Figure 6B is reproduced with permission from ref 229. Copyright 2017 Wiley.

When a sufficiently strong Lewis acid is used (e.g., Sc^{3+}) with an analogous TAML system lacking the peripheral pyridine motif, binding of redox-inactive ions is proposed to occur at the one of the amide carbonyl moieties of the macrocyclic ligand (**23-Sc**; Figure 5A).[152] Binding of Sc^{3+} greatly increases the rate (>10^4) of oxygen atom transfer to PPh_3 and shifts the potential for oxidation by ∼0.70 V as measured via spectrophotometric titration. In a related Co^{III}–oxyl complex, binding of Sc^{3+}, Ce^{3+}, Y^{3+}, and Zn^{2+} is proposed to occur at the Co–oxo moiety.[151] This binding results in valence tautomerism to a [Co^{IV}–O–M^{n+}] species (**24**, Figure 5A) and in acceleration of OAT rates to thioanisoles, with the more Lewis acidic ions engendering the largest rate acceleration.[151]

Oxygen atom transfer from multimetallic clusters has also been reported. The well-defined nature of these clusters is a key advantage in studying the effects of redox-inactive metals on reactivity over strategies that rely on dynamic binding of Lewis acidic metal ions in solution. Heterometallic cubane clusters [LMn_3MO_4] (**10-M**; M = Sc^{3+}, Mn^{3+}, Gd^{3+}, Co^{3+}) react with trimethylphosphine (PMe_3) to generate the corresponding trioxo complexes [LMn_3MO_3] via transfer of a single O atom to PMe_3. The most Lewis acidic apical metal (Mn^{3+}) displayed the fastest rate of OAT. Intriguingly, the oxidation state of the basal manganese metal centers also influenced the rates of OAT: whereas OAT occurs readily with complexes possessing [$Mn^{III}Mn^{IV}_2$] core, $1e^-$ oxidation to [Mn^{IV}_3] shuts down oxygen atom transfer almost completely, even in the presence of strongly Lewis acidic Sc^{3+}. Computational studies revealed large kinetic barriers to dissociation of bridging carboxylates from Mn^{IV} ions. Since carboxylate dissociation is required for substrate access to the cluster O atoms and was calculated to be the first step of the OAT process, slower dissociation rates unsurprisingly lead to slower OAT processes. Labeling studies with ^{18}O confirmed that OAT occurs from one of the "top" μ_3-oxygen atoms—near the dissociating carboxylate on the cubane face—and that the resulting trioxo species are structurally dynamic, resulting in ^{18}O scrambling and isolation of complexes in which the "empty" oxo site is located at the bottom of the cluster.

The more oxidizing oxo-hydroxo clusters **11-M** exhibited much faster rates of OAT. Similar to their cubane analogues, these clusters displayed OAT rates that were dependent on the Lewis acidity of the redox-inactive metal, where the most Lewis acidic metal (Y^{3+}) displayed faster rates of phosphine oxidation. It is perhaps unsurprising that these tetranuclear metal complexes display faster OAT, since the μ_2-oxygen atom is much more accessible and does not require dissociation of any additional ligands. In contrast to the cubane series, however, oxygen atom transfer is not reversible in these metal clusters, and the metal-containing products of these reactions were not characterized. OAT reactivity of the corresponding iso-structural iron complexes (**12-M**) was analogously affected by the Lewis acidity of the redox-inactive metal[111]. Overall, when comparing Fe_3 and Mn_3 complexes that incorporate redox inactive metals of similar Lewis acidity (e.g., Gd^{3+}, Y^{3+}, or La^{3+}, which possess similar metal–aqua pK_a's) OAT reactivity is in line with the one-electron reduction potentials of the metal clusters, with more positive reduction potentials correlating with faster OAT rates, though not sufficiently oxidizing to support single electron transfer chemistry.[111]

As indicated by the reports highlighted in this section, the OAT reactivity of redox-active complexes in the presence of Lewis acidic additives has been studied extensively, with clear correlations emerging between reaction rates and Lewis acidity, providing a key tool for modulating the reactivity of high-valent metal complexes in O atom transfer reactions. As binding of cations to metal–oxo motifs results in marked effects on reduction potential, significant shifts are often engendered in the mechanism of group transfer reactions and dramatic effects on rate have been observed. Many of the discussed transformations for which mechanistic studies are available, including thioanisole and phosphine oxygenation, share a similar rate-determining step, MCET, that is analogous to well-established PCET processes. These results highlight the ability of redox-inactive moieties to profoundly affect the transfer of oxygen atoms even without direct participation in the transfer of electrons.

https://doi.org/10.1021/jacsau.3c00675
JACS Au 2024, 4, 344–368

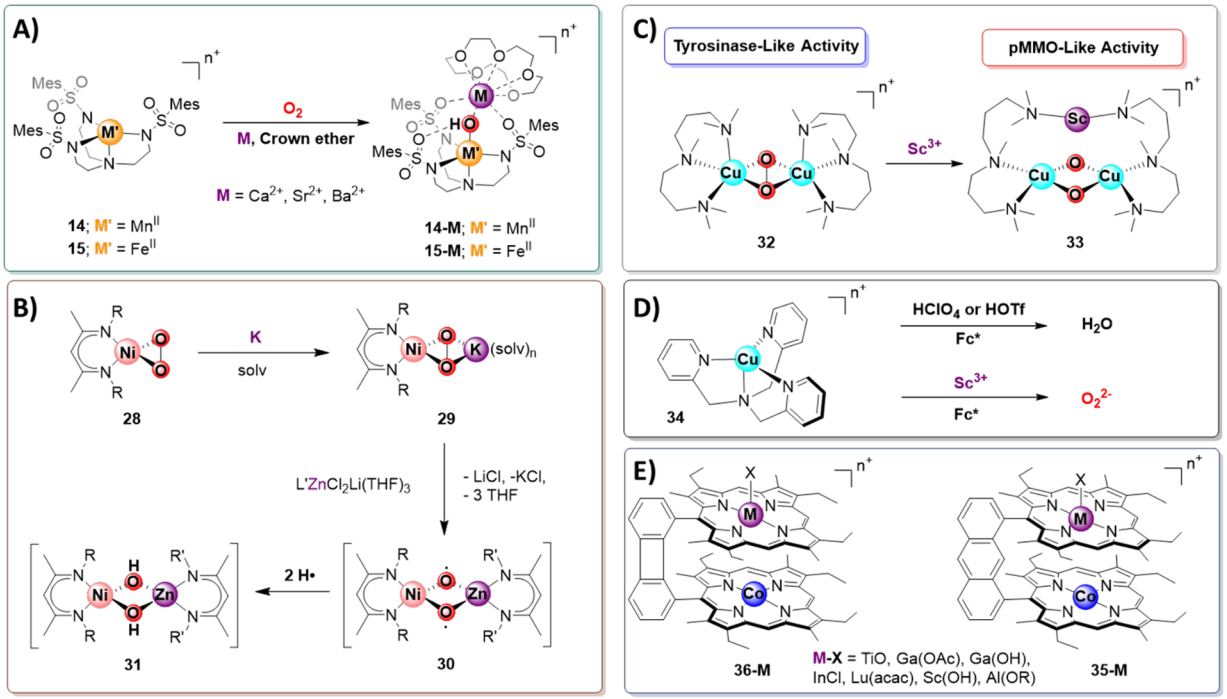

Figure 7. Heterobimetallic effects in the activation of dioxygen. (A) Reactivity of complexes **14** and **15** with dioxygen in the presence of redox-inactive metals. (B) Formation of complex **31**, upon reduction of superoxo species **28** with potassium metal, followed by transmetalation by zinc. (C) O−O bond cleavage in **32** mediated by Sc^{3+}. (D) Reactivity of monometallic copper complex **34** with dioxygen in the absence and presence of Sc^{3+}. (E) Heterobimetallic Co porphyrin complexes with a variety of bound redox-inactive metals, based on bis-porphyrin scaffold with a biphenylenyl (**36-M**) and anthracene (**35-M**) backbone.

4. LEWIS ACID EFFECTS ON O_2 ACTIVATION

Electron transfer coupled with dioxygen activation frequently results in the formation of highly reactive metal−superoxo, −peroxo, or −oxo species within the active sites of many enzymes.[3,196−201] As a result, significant efforts have been undertaken to synthesize metal complexes that bear such moieties in order to better understand the chemistry behind activating and/or breaking the O−O bond.[9,15−17,127,128,134,136,139−141,143,144,202−220] As discussed for ET and OAT, Lewis acids can significantly influence the chemistry behind dioxygen activation. For instance, it has been demonstrated that many Lewis acids can form adducts with the superoxide ($O_2^{\bullet-}$) anion in solution.[221,222] Binding of Lewis acids to this radical anion promotes electron transfer from metal complexes to O_2, a process that has been extensively investigated using [(TPP)Co^{II}] (TPP = tetraphenylporphyrin dianion) as the reductant.[62,223] In the absence of Lewis acids, [(TPP)Co^{II}] does not engage in ET with O_2, in good agreement with its positive reduction potential (E_{ox} ([(TPP)-$Co^{III/II}$]) = 0.35 V, E_{red} ($O_2^{0/\bullet-}$) = −0.86 V vs SCE).[223,224] Addition of redox-inactive metal salts (e.g., Sc^{3+}) results in $1e^-$ reduction of O_2 as monitored by UV−vis and EPR spectroscopies. The rate of electron transfer increases dramatically as the Lewis acidity of the metal-ion is increased. A plot of log(k) vs metal−superoxide binding energy reveals a striking linear correlation, which highlights the rate-accelerating effects of stronger binding of M^{n+} ions to superoxide.[62,223,225] Similar effects have been observed in ET between metal complexes and organic electron acceptors (e.g., quinones).[62] As a result of these studies, the metal−superoxide binding energy has been implemented as a quantitative measure of Lewis acidity in many subsequent investigations especially by the groups of Fukuzumi and Nam.[55,62,149,153,159,160,184,221,223,226−230]

Lewis acids also coordinate directly to metal−superoxo, and −peroxo species, facilitating their isolation and characterization.[231−234] In particular, the reactivity of metal−peroxo complexes with the TMC ligand has been investigated (Figure 6).[227−229,235,236] It has been shown that superoxide complex [(TMC)Fe^{III}−($O_2^{\bullet-}$)] (**26**) is metastable in solution, but decays to Fe−oxo complex [(TMC)Fe^{IV}(O)] (**27**) in the presence of both a reducing agent and a source of protons (Figure 6).[237] Similar reactivity can be induced by Lewis acids (Sc^3 or Y^{3+}) in the presence of a reducing agent (Ph_4B^- or Fc).[227,236] Upon conversion to **27**, a distinct intermediate was observed by UV−vis spectroscopy that is stable at −40 °C for several days. Based on characterization via Raman, EPR, ESI-MS, and EXAFS spectroscopy, this intermediate was unequivocally assigned as Fe^{III}−(μ−η^2:η^2-O_2^{2-})−M^{3+} (**26-M**, M = Sc or Y), where the Lewis acid is bound in a side-on fashion to the metal−peroxo moiety. Binding of the Lewis acid is crucial for the observed reactivity: in the absence of Lewis acids, reduction of **26** does not lead to O−O bond cleavage and formation of the high-valent Fe^{IV}-oxo species.[227,236] The rate of reduction is dependent on the nature of the Lewis acid, as the more Lewis acidic Sc^{3+} reacts three times faster than the corresponding Y^{3+} analogue. Furthermore, screening of a series of reductants shows that the ET reorganization energy is not affected by the presence of a second metal ion, indicating that the differences in ET rate between **26** and **26-M** are derived solely from the positive shift in reduction potential (estimated from the same analysis to be ∼0.24 V).

In subsequent studies, the reactivity and redox properties of complexes **25** and **26** were reported in further detail.[228,229] It

https://doi.org/10.1021/jacsau.3c00675
JACS Au 2024, 4, 344−368

was found that upon photoirradiation of an O_2-saturated solution containing **25**, dimeric *N*-benzyl-1,4-dihydronicotinamide [$(BNA)_2$], and a redox-inactive metal salt, different products are formed depending on the nature of the added Lewis acid.[228] With Ca^{2+} and Sr^{2+}, the Lewis acid-bound iron-peroxo species **26-M** is formed, whereas with Zn^{2+}, Lu^{3+}, Y^{3+}, and Sc^{3+} the high-valent iron-oxo species **27** is generated. As previously discussed, the latter species is only formed after reduction of [(TMC)$Fe^{III}(O_2^{\bullet-})$], which is followed by O−O bond cleavage.[227,236] Clearly, the redox properties of the intermediate **26-M** are modulated by the Lewis acid. These observations are consistent with the 1e$^-$ reduction potentials of the independently synthesized complexes **26-M**, which correlate linearly with the Lewis acidity of the redox-inactive metal ions (see Section 2). Addition of [$(BNA)_2$)] to these complexes resulted in reduction of **26-M** only when M = Zn^{2+}, Lu^{3+}, Y^{3+}, or Sc^{3+}, establishing that the Lewis acidity of the redox-inactive metal directs the reactivity of complex **25**.[228,229]

An effect of Ca^{2+} and Sr^{2+} on dioxygen activation was observed in Fe and Mn complexes supported by the MST tripodal framework (**14** and **15**, respectively).[122,123] In the absence of any additives, O_2 activation by these complexes is sluggish and no oxidized species could be isolated following treatment with O_2. Upon addition of Group 2 metals, remarkable rate enhancements were observed for Ca^{2+} and Sr^{2+} (∼30−40-fold), whereas for Ba^{2+}only modest (∼10−20-fold) rate enhancements were observed. A clear difference between Fe and Mn complexes was also noted, as the rate of dioxygen activation differs by 1 order of magnitude in favor of Fe.[122,123] In this system, the role of the secondary coordination sphere is pivotal in the rate acceleration by these Lewis acids. Not only do the sulfonamido moieties serve as hydrogen bonding acceptors to the generated M^{III}−OH species (M = Mn and Fe), but they can also coordinate the group 2 metal ions, establishing a unique M^{II}−(μ-OH)−M' core (M = Fe and Mn, and M' = Ca^{2+}, Sr^{2+}, and Ba^{2+}) that is in several aspects akin to the OEC (Figure 7A). It is proposed that initial binding of these Lewis acids to [M^{II}MST]$^+$ complexes facilitates electron transfer to O_2, generating an intermediate M^{II}−(superoxo)−M' species, which−via multiple steps−decomposes to the final M^{III}−OH species.[123] Although no definite experimental evidence is provided for the existence of such superoxo intermediates, the Lewis acid-induced rate enhancements are consistent with the previously discussed 1e$^-$ O_2 activation by cobalt porphyrin complexes in the presence of Lewis acids (*vide supra*), where superoxo intermediates have unequivocally been identified.[62,223] Cobalt complexes supported by analogous ligand scaffolds have also appeared in the literature, although no reactivity with O_2 was reported.[238]

Addition of redox-inactive metals has also been observed to affect the reactivity of other metal−peroxo and −hydroperoxo species. Peroxo-cobalt(III) compound [Co^{III}((TBDAP)-(O_2^{2-})]$^+$ (TBDAP = *N*,*N*′-di-*tert*-butyl-2,11-diaza[3.3](2,6)-pyridinophane) reacts with nitriles to form a hydroximato species. In the presence of redox-inactive metals a peroxyimidatocobalt(III) species is isolated instead,[239] and the logarithm of the rate of this reaction is linearly correlated to the Lewis acidity of the redox-inactive metals. In contrast, more Lewis acidic trivalent redox-inactive metals were found to hinder nucleophilic reactivity of a separate alkylperoxocopper-(II) system with cyclohexylcarboxaldehyde.[240] Addition of Sc^{3+} (or $HClO_4$) also enables rapid hydroxylation of cyclohexane and benzene by a mixture of [Fe(β-BPMCN)$(CH_3CN)_2$]$^{2+}$ (BPMCN = N,N′-bis(pyridyl-2-methyl)-N,N′-dimethyl-trans-1,2-diamino-cyclohexane) and H_2O_2, for which it is hypothesized that the Lewis acidic additives enhance O−O bond cleavage to yield a highly reactive Fe^{V}−oxo intermediate.[241]

Activation of O_2 with complexes that form distinct homobimetallic [M−(μ-O)$_2$−M] cores (M = Fe, Ni, and Cu) have been extensively investigated, and their chemistry has been described in a series of excellent reviews.[3,9,16,17,207,211,213,214,216,242] Heterobimetallic examples are more rare,[15,243,244] especially those containing redox-inactive metals.[245] A prominent example is the μ−η^2:η^2-peroxo-bridged β-diketiminate (L) complex [LNi−(O_2)−K$(THF)_n$] (**29**), generated upon reduction of the superoxo complex [$LNiO_2$] (**28**) with potassium metal.[245] While nickel−potassium complex **29** is a stable peroxide species, transmetalation of potassium with the more Lewis acidic Zn^{2+} (supported by an additional diketiminate ligand) results in fast H atom abstraction to generate the complex [LNi−(μ-OH)$_2$−ZnL] (**31**), featuring two bridging hydroxide ligands. The differences in reactivity between complex **29** and the putative [LNi−(O_2^{2-})−ZnL'] (**30**) intermediate generated upon addition of [LZn^{2+}] were explained based on DFT calculations. For peroxo complex **30**, a triplet ground state was predicted with significant spin density on the bridging oxo-ligands, indicating (at least partial) O−O bond scission. In contrast, the O−O bond in **29** remains intact, and the ground state is a singlet. Exchange of K^+ for the more Lewis acidic Zn^{2+} thus results in a higher degree of O_2 activation, from (μ-O_2^{2-}) to (μ-O^{2-})$_2$, generating a [LNi−(O)$_2$−ZnL] intermediate, which is only transient and rapidly undergoes HAT (from the solvent or other exogenous sources) to give **30**. Replacement of Zn^{2+} in these systems with Fe^{2+}, Co^{2+}, Ni^{2+}, or Cu^{2+} resulted in nucleophilic reactivity pathways (vs electrophilic reactivity for Zn),[246−248] highlighting that despite similar Lewis acidities (see Table 1), redox-inactive metals can engender distinct reactivity manifolds from their redox-active counterparts in dioxygen transformations including O−O bond cleavage.

In a related dinuclear copper system, the degree of O_2 activation was also found to be dependent on the presence of Lewis acid ions.[249] Exposing [(MeAN)Cu^{I}][BAr^{F}_4] (MeAN = *N*-methyl-*N*,*N*-bis[3-(dimethylamino)propyl]amine) to O_2 at low temperatures results in formation of a stable peroxo−dicopper(II) complex (**32**). Complex **32** displays a characteristic [M−(μ-O_2^{2-})−M] core and exhibits no discernible reactivity toward external substrates.[250] However, in the presence of Sc^{3+}, **32** generates a species whose spectroscopic features are consistent with a dioxo-bridged copper(III) dimer (**33**), where the O−O bond has been fully cleaved.[249] The presence of the well-precedented [Cu^{III}−(μ-O)$_2$−Cu^{III}] core was confirmed by resonance Raman spectroscopy and supported by DFT calculations. In contrast to several of the previously discussed peroxo- and bis-μ-oxo-complexes, in which coordination of the relevant redox-inactive metal ions to the O_2-derived ligands is typically observed, calculations on this dicopper system suggested that scandium does not coordinate via the oxygen atoms, but rather to one nitrogen donor from each MeAN ligand.[249] Sc^{3+} coordination thus promotes dissociation of one of the nitrogen ligands from copper, resulting in a change in the coordination geometry at Cu (Figure 7B). This change influences the orbital overlap between the MeAN nitrogen donors and the copper d-orbitals; the resulting increase in electron density at Cu enables a higher degree of backbonding to the σ* orbitals on the O_2^{2-} motif,

https://doi.org/10.1021/jacsau.3c00675
JACS Au 2024, 4, 344−368

which facilitates O−O bond scission. A unique feature of this system is that the O−O bond can be reformed upon sequestering the Lewis acid with other bidentate, nitrogen-based ligands, restoring the original coordination geometry of the copper complex. Along with influencing the reversible formation and cleavage of the O−O bond, the binding of Sc^{3+} also alters the reduction potential of the dioxo-bridged copper(III) complex **33**, which in contrast to peroxo-dicopper(II) complex **32**, is more reactive toward weak C−H and O−H bonds.[249]

In other copper complexes, oxygen reduction to water (a $4e^-$ process) or to peroxide (a $2e^-$ process) can be regulated by a variety of redox-inactive metal ions.[251] In the absence of a Lewis acid, O_2 reduction to H_2O was observed with $[(tmpa)Cu^{II}(MeCN)][ClO_4]_2$ (**34**; tmpa = tris(2-pyridylmethyl)amine) in the presence of decamethylferrocene (as sacrificial reductant) and triflic acid (as H^+ source; Figure 7D). This four-electron reduction process proceeds via the $[(tmpa)Cu^{II}(O_2^{2-})Cu^{II}(tmpa)]^{2+}$ peroxide intermediate.[252] Performing the same reaction in the presence of Sc^{3+} does not yield H_2O; rather, formation of a $[Sc(O_2^{2-})]^+$ species is indicated by EPR spectroscopy.[251] Kinetic studies suggest that, unlike in the case of O_2 reduction to water, no bis(copper(II))−peroxo dimer is formed, and a monomeric superoxo−copper complex $[(tmpa)Cu^{II}(O_2^{\bullet-})]^+$ is generated instead.[251] This copper(II)−superoxo complex is rapidly reduced by decamethylferrocene in the presence of Sc^{3+} to produce $[Sc(O_2^{2-})]^+$ and regenerate **34**. Other Lewis acids also facilitate an analogous two-electron reduction to the corresponding metal−peroxide. The rates of these reactions correlate with the Lewis acidity of the redox-inactive metal, where the most Lewis acidic metal ion gave the highest activity.[251] A quantitative measure of these effects (e.g., a linear correlation), however, could not be generated due to the absence of quantitative rate data in the original publication.

Analogous four- and two-electron reduction processes involving dioxygen were also investigated with a series of a cofacial bisporphyrin "Pacman" complexes containing one Co^{II} center to enable dioxygen binding, along with a Lewis acidic metal in the second porphyrin to control O_2 reduction chemistry (**35-M** and **36-M**, Figure 7E).[253,254] The catalytic activity of each heterobimetallic complex was compared to that of the known homobimetallic catalyst bisporphyrin−Co_2, which facilitates the $4e^-$ reduction of O_2 to H_2O.[255] It was proposed that, in this system, dioxygen binds to the mixed valent state of the catalyst (bisporphyrin−$Co_2^{III}Co^{II}$) at the Co^{II} center, and that the second Co site (Co^{III}) acts as a Lewis acid to facilitate the overall reductive transformation. The reactivity of the isostructural heterobimetallic complexes was studied by rotating-disk voltammetric methods;[253] from these studies, complexes **35-M** (M = Ti^{4+}, Ga^{3+}, In^{3+}, Lu^{3+}, Sc^{3+}) were found to reduce dioxygen at potentials close to that for Co−monoporphyrin at +0.55 V (vs NHE), with a limiting current indicating a two-electron mechanism.[253] In contrast, complexes **35-Lu**, **36-Lu**, and **36-Sc** reduce dioxygen at a potential close to +0.7 V (∼100 mV more negative compared to the homometallic $[Co]_2$ catalyst and 300 mV more positive than a Co−monoporphyrin complex). Moreover, their limiting currents are larger than those observed for the Co−monoporphyrin, and only slightly smaller than for the $[Co_2]$ complex. Taken together, these observations suggest that, while bisporphyrin−Co_2 selectively reduces O_2 by four-electrons to generate H_2O, **35-Lu**, **36-Lu**, and **36-Sc** might reduce O_2 via two concurrent but separate 2- and $4e^-$ mechanisms to produce H_2O_2 and H_2O, respectively. H_2O_2 was indeed detected at the ring electrode upon dioxygen reduction in the latter cases, providing additional support for the operability of the $2e^-$ pathway.[253] Together with the nature of the Lewis acid, the distance between the metal centers in these bimetallic assemblies also appears to be an important factor. While the identity of the redox-inactive metal played a key part in the observed transformations, the exact role of these metal ions in directing reactivity and enabling different mechanistic pathways for O_2 reduction (e.g., 4- vs $2e^-$ reduction) remains unclear. These studies nonetheless demonstrate that, together with accelerating O_2 activation, Lewis acidic metal ions are also able to control mechanistic aspects of O_2 reduction, engendering a shift between four- and two-electron reduction processes.

5. LEWIS ACID EFFECTS ON O_2 EVOLUTION

The role of Lewis acids in O_2 evolution is a fundamental aspect of the mechanism of water oxidation by the OEC,[67,256−258] which contains calcium and manganese ions ($CaMn_4O_4$) in a cuboidal arrangement in its active site.[132,259−263] The influence of Lewis acids on water oxidation has mainly been studied on heterogeneous surfaces of mixed-metal oxides, which have attracted significant interest as promising water oxidation catalysts.[264] In 2008, a heterogeneous cobalt-oxide water oxidation catalyst was reported that self-assembles from Co^{II} ions in solution.[265] Energy-dispersive X-ray (EDX) analysis of the electrodeposited film indicated that, besides cobalt, potassium and phosphate are also present in substantial amounts. Based on additional X-ray absorption near-edge structure (XANES) and extended X-ray absorption fine structure (EXAFS) studies, it was suggested that potassium might be involved in forming distinct KCo_3O_4 cubanes,[266] although other studies have debated such a role for potassium.[267] The influence of redox-inactive metals on water oxidation has been studied more extensively in manganese oxides that are structurally similar to the birnessite family of minerals.[36−40] These manganese oxides form layers of edge-sharing MnO_6 octahedra, in which redox-inactive metals can intercalate.[37] Studies on these synthetic mixed-manganese oxides revealed that, in the presence of redox-inactive metals, a marked increase in O_2 evolution was observed compared to plain manganese oxide.[36,37] The O_2 evolution activity followed the trend $Ca^{2+} > Sr^{2+} \gg Mg^{2+} \sim Na^+$, very similar to the activity profile of the OEC. A similar trend was also observed upon incorporating Ca^{2+} and Sr^{2+} in polymeric cobalt cyanide complexes.[268] Computational studies into the electronic structure of various redox-inactive metal-substituted birnessites suggested that a suitable band gap for water splitting was observed when Ca^{2+} or Sr^{2+} were intercalated between the manganese oxide layers.[269] Incorporation of redox-inactive metals into Ni−Fe oxides have also been demonstrated to enhance their water oxidation capabilities.[270,271]

In contrast to heterogeneous materials, fewer reports have described in detail the effects of Lewis acids on O_2 evolution from molecular complexes. In one of the few detailed studies, the role of Ca^{2+} and Sr^{2+} in enabling O_2 evolution from Fe−peroxide complexes **26-M** was investigated. As discussed in Section 2, potentials required for both reduction and oxidation of complexes **26-M** depend on the Lewis acidity of the redox-inactive metal M; while reductive reactivity, facilitated by *more* Lewis acidic cations (Zn^{2+}, Lu^{3+}, Y^{3+}, Sc^{3+}), leads to generation

https://doi.org/10.1021/jacsau.3c00675
JACS Au 2024, 4, 344−368

of Fe^{IV}−oxo complex **27**, oxidation of **26-M** is inaccessible at moderate potentials except in the presence of the *less* Lewis acidic cations Ca^{2+} and Sr^{2+}. Such a unique behavior for Ca^{2+} and Sr^{2+} is reminiscent of the OEC in PSII, where only in the presence of these two redox-inactive metals is O_2 evolution observed.[258] However, as Fe^{III}−peroxide complex **26** can also be oxidized to release O_2 in the absence of *any* redox-inactive metals, it is possible that both in these systems and in the OEC, the reduction potentials engendered by Ca^{2+} and Sr^{2+} for complex/cluster oxidation are sufficiently negative as to not *prevent* O_2 release, rather than actively *promote* it.[228]

In an attempt to further elucidate the factors governing the structure and reactivity of the OEC, the effects of water coordination to redox inactive metals in **26-M** (M = Ca^{2+}, Zn^{2+}, and Sc^{3+}) were investigated,[235] as water is known to play a prominent role in the primary coordination sphere of the OEC.[132,259−263] Addition of water (0−2.8 M) to **26-Zn** resulted in a marked change in the UV−vis spectrum of the complex that was found to be consistent with binding of two water molecules to Zn^{2+}. A similar value was found for Ca^{2+} but not for Sc^{3+}, where addition of water resulted in formation of redox-inactive metal-free **26**, indicating loss of Sc^{3+} The coordination of water to Zn^{2+} had marked effects on the physicochemical properties of the resulting iron−peroxo species $[(TMC)Fe^{III}-(\mu-\eta^2:\eta^2\text{-}O_2)-Zn^{2+}(OH_2)_2]$.[235] Most notably, the binding of water resulted in a decrease of the Lewis acidity of Zn^{2+}, estimated from the g_{zz} values determined by EPR spectroscopy in accordance with the previously utilized approach for determination of Lewis acidities by EPR.[62] The "observed" Lewis acidity for Zn^{2+} under these conditions in the presence of water (0.57 eV), is more in line with those reported for Ca^{2+} (0.59 eV) and Sr^{2+} (0.53 eV), and is reflected in the reactivity $[(TMC)Fe^{III}-(\mu-\eta^2:\eta^2\text{-}O_2)-Zn^{2+}(OH_2)_2]$, which is akin to that observed for $[(TMC)Fe^{III}-(\mu-\eta^2:\eta^2\text{-}O_2)-Ca^{2+}]$ (**26-Ca**): indeed, while CAN does not oxidize $[(TMC)Fe^{III}-(\mu-\eta^2:\eta^2\text{-}O_2)-Zn^{2+}]$ to give **25** and O_2, $[(TMC)Fe^{III}-(\mu-\eta^2:\eta^2\text{-}O_2)-Zn^{2+}(OH_2)_2]$ readily evolves one equivalent of O_2 upon one-electron oxidation. The coordination of water thus modulates the Lewis acidity of Zn^{2+} leading to a change in the redox properties of the corresponding iron−peroxo complex, resulting in reactivity that is analogous to that reported for the related Ca^{2+} and Sr^{2+} complexes in the absence of coordinated water.[235] Coordination of water also induces a negative shift in the reduction potential of $[(TMC)Fe^{III}-(\mu-\eta^2:\eta^2\text{-}O_2)-Zn^{2+}(OH_2)_2]$, and results in lower ET rates from 1,1′-dimethylferrocene. It is remarkable that a single system has been successfully leveraged to probe both the influence of redox−inactive metals and of water in the (secondary) coordination sphere on both O_2 activation and evolution, all factors and contexts that are proposed to be highly relevant in tuning the structure and reactivity of the OEC in PSII.

The effect of Group 2 metals on O_2 evolution by the inorganic oxidant potassium ferrate (K_2FeO_4) has also been studied. At low pH, potassium ferrate readily oxidizes water to dioxygen, in part due to its positive potential for oxidation.[272,273] The stability of K_2FeO_4 is pH dependent,[272,273] and at pH 9−10 minimal decomposition is observed (2% h^{-1}) in the absence of any redox-inactive metal additives.[274] However, addition of excess Ca^{2+} to solutions of K_2FeO_4 at pH 9−10 resulted in O_2 evolution from the reaction mixture. Substituting Ca^{2+} for Sr^{2+} or Mg^{2+} did not change the yield or kinetics of the O_2 evolution reaction. A DFT study into the mechanism of this reaction suggests mainly a structural role for Ca^{2+} (or Sr^{2+} or Mg^{2+}), where a bound Ca^{2+} ion bridges two ferrate anions, bringing two distinct oxygen substituents in close proximity, facilitating O−O bond formation, a mechanism supported by isotopic labeling experiments. A similar mechanism was proposed for water oxidation by K_2FeO_4 under acidic additions, as proton-induced dimerization of FeO_4^{2-} results in O_2 evolution.[272]

Overall, even the limited studies that are available suggest that Ca^{2+} and Sr^{2+} occupy a special niche in facilitating O_2 evolution, consistent with observations of the OEC, and a growing body of work has begun to outline the potential modes of their participation in this key transformation. Nonetheless, additional studies are necessary both on synthetic complexes and on the OEC itself to further elucidate the exact role that these metal ions surprisingly have on O_2 evolution.

6. LEWIS ACID EFFECTS ON HYDROGEN ATOM TRANSFER

H atom transfer (HAT) reactions are closely linked to O_2-derived reactivity, including biologically essential organic substrate activation by metal-oxo species. HAT reactions represent another set of processes on which heterometallic effects have been extensively investigated. Many of the complexes described in the previous sections are also active for HAT, and where appropriate some of the effects of redox-inactive metals have already been alluded to in conjunction with their other properties. A handful of additional systems have not yet been discussed and will be the focus of this section.

Fe^{III}−peroxo complexes **26-M** have already been discussed in the context of both ET (Section 2) and O_2 activation (Section 4). Further investigations into these complexes also revealed remarkable linear correlations between the Lewis acidity of the redox-inactive metal and the activity of these complexes in HAT reactions, as well as in aldehyde deformylation.[229] Notably, plots of log(k) for various transformations (ET, HAT, aldehyde deformylation) vs Lewis acidity reveal linear correlations (Figure 6B); furthermore, the slope of the linear fit in these correlation plots indicates the direction of charge transfer: reactions proceeding via electrophilic mechanisms (ET and HAT) produce a positive slope, whereas nucleophilic mechanisms show the opposite trend.[229]

In the series of complexes of the pentadentate ligand dpaq $[(dpaq)Mn^{IV}O]^+-M^{n+}$ (**19- M**, M = Ca^{2+}, Mg^{2+}, Zn^{2+}, Lu^{3+}, Y^{3+}, Al^{3+}, Sc^{3+}; Figure 3) discussed in Section 2, contrasting observations were reported on the effects of Lewis acidity on the rate of ET/OAT vs HAT reactions. Specifically, while the rate of ET and OAT reactions displayed a linear, positive correlation with Lewis acidity, HAT rates *decreased* with increasing Lewis acidity. These results were taken as an indication that the Lewis acidity of the redox-inactive metal is involved in modulating the *basicity* of the metal−oxo moiety. The more Lewis acidic ions make the Mn−oxo motif less basic, affecting the concerted HAT to the oxo-motif, resulting in an overall slower reaction. On the other hand, reactions in which HAT proceeds via an initial ET step due to increased driving force for ET, and for which ET is therefore rate-determining, become faster as the reduction potential of the complex shifts to more positive values (i.e., with more Lewis acidic ions).[159] Analogous studies with triflic acid (HOTf), while not involving redox-inactive metals, further indicate that interactions between the Mn−O moiety and Lewis acidic centers (H^+ or

https://doi.org/10.1021/jacsau.3c00675
JACS Au 2024, 4, 344−368

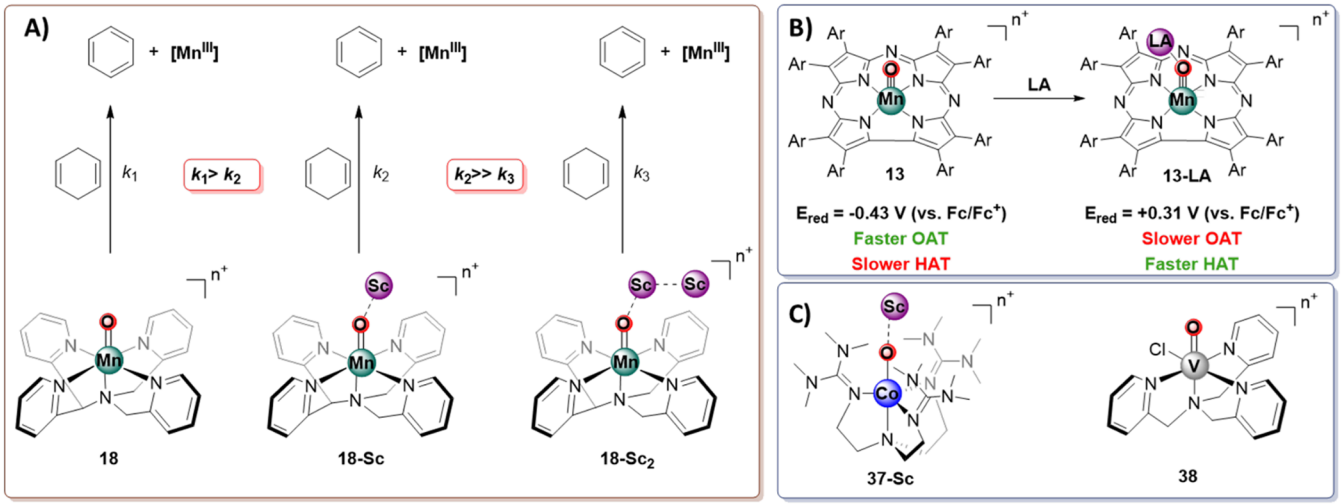

Figure 8. Hydrogen abstraction properties of various metal complexes upon binding redox inactive metals. (A) Differences in the rate of hydrogen atom abstraction from cyclohexadiene with complex **18** upon binding of one and two scandium ions. (B) Reactivity trends of a manganese corrolazine complex in oxygen atom (OAT) and hydrogen atom transfer (HAT) reactions in the absence (**13**) and presence of Lewis acids (**13-LA**; LA = $B(C_6F_5)_3$, HBF_4, and $Zn(OTf)_2$). (C) Cobalt and vanadium complexes involved in HAT reactions.

M^{n+}) modulate the chemical and physical properties of the Mn−O group.[230] It should be noted that the assignment of the active species in these studies as $[(dpaq)Mn^{IV}O]^+$−M^{n+} (with Lewis acidic ions interacting directly with the metal−oxo moiety) has recently been challenged for room-temperature studies on the basis of ^1H NMR and electronic absorption spectroscopies, concurrent with a proposed new role for redox-inactive metal ions in promoting protonation of the precursor $[(dpaq)Mn^{III}(OH)]^+$ complex to the corresponding aqua complex $[(dpaq)Mn^{III}(OH_2)]^{2+}$.[275]

The effects of redox-inactive metals on HAT by Mn complex **18** were studied in more detail than for the isostructural Fe complex **17** (Figure 8).[165] While the addition of Sc^{3+} to **18** resulted in an increase in the rate of OAT, the opposite effect is observed for H atom transfer, where binding of Sc^{3+} results in a decrease in reaction rate. Reaction of **18** with 1,4-cyclohexadiene (CHD) was found to be 5 and 180 times faster than for its 1:1 and 1:2 Sc^{3+} adducts **18-Sc** and **18-Sc$_2$**, respectively.[165] This change in reactivity is ascribed to the different steric requirements for the two reactions. As determined via kinetic studies, OAT reaction rates correlate with the ET driving force−i.e. OAT to thioanisole proceeds via a rate-determining ET step.[146] This step is largely uninfluenced by the steric constraints imposed by Sc^{3+} binding, and is followed by a fast O atom transfer. In the case of H atom transfer, however, significant interaction between substrate and Mn−O species is proposed to be necessary, and binding of Sc^{3+} sterically hinders this interaction leading to reduced reaction rates.[165] A HAT mechanism is thus proposed for **18**, yet no kinetic isotope effects are reported for the reaction of **18** with CHD, so a classical HAT step might not be rate-determining.

In contrast, studies with complex **17** have mainly focused on C−H bond cleavage in toluene derivatives.[184] Complex **17** itself only displayed slow reactivity with toluene analogues, and the large kinetic isotope effect (KIE = 31) suggested a classical H atom transfer mechanism followed by oxygen rebound to yield benzylic alcohols. Addition of $Sc(OTf)_3$ resulted in ∼2−100-fold increase in observed reaction rates.[184] In parallel work using the HOTf in place of $Sc(OTf)_3$, small KIEs were observed at high concentrations of HOTf, indicating a shift in mechanism.[184] As for the OAT to thioanisole (*vide supra*), this new mechanism is believed to involve ET-OT steps, and the reaction rate is thus not susceptible to the sterically hindered environment around the Fe−oxo moiety, as the ET step is likely rate-determining. Interestingly, a shift in mechanism was also observed in the oxidation of a variety of benzyl alcohols. Addition of Sc^{3+} to **17** results in a 120-fold increase in the rate of oxidation of 2,5-dimethoxybenzyl alcohol without any observable KIE. Indeed, mechanistic studies confirmed that this reaction proceeds via a rate-limiting ET step. On the other hand, reduction of benzyl alcohols with more positive oxidation potentials proceeded with large KIEs, suggesting HAT as the rate-determining step. Consequently, the overall mechanism of benzyl alcohol oxidation depends on the oxidation potential of the substrate and discriminates between HAT and PCET (or MCET) pathways.[276] Unfortunately, a direct comparison with the HAT properties of **18** is not possible, since hydrogen atom abstraction from CHD with complex **17** is not reported.[184]

More detailed studies into the hydrogen atom abstraction reactivity with complexes **13** and **13-Zn** were also performed (Figure 8).[277] Addition of xanthene (BDE = 74 kcal mol^{-1}) to complexes **13** and **13-Zn** resulted in rapid formation of $[(TBP_8Cz)Mn^{IV}(OH_2)]$ and $[(TBP_8Cz)Mn^{IV}(OH)]$, respectively. A clear difference is thus observed upon coordination of Zn to **13**. Whereas for **13** two H atom transfers are observed, only a single H atom transfer is reported for **13-Zn**. It is proposed that binding of Zn^{2+} to Mn^{IV}−OH species generated by an initial HAT process prevents transfer of a second hydrogen atom. A 4-fold enhancement of reaction rate is also observed upon Zn binding.[277] Rate enhancements were also observed upon addition of other Lewis acids such as $HBAr^F_4$ and $B(C_6F_5)_3$. Kinetic studies revealed that H atom abstraction is the rate-limiting step in the reaction of xanthene with **13** and **13-LA**, as both displayed large kinetic isotope effects (KIE = >20; LA = $HBAr^F_4$ or $B(C_6F_5)_3$). Compared to **18-M**, steric inhibition by the Lewis acids complexes **13-M** is negligible.[277]

A direct HAT mechanism was also proposed for **24-Sc** in the presence of xanthene, 9,10- dihydroanthracene (BDE = 76 kcal

https://doi.org/10.1021/jacsau.3c00675
JACS Au 2024, 4, 344−368

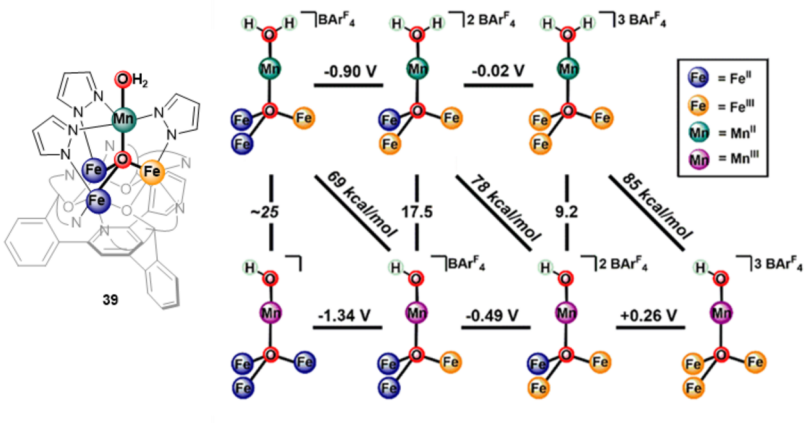

Figure 9. Redox state of remote cations affect HAT reactivity of metal-oxo clusters. Oxidation state and charge of remote Fe_3 sites have significant effect on HAT reactivity of terminal Mn−OH_2 moiety. Figure reproduced from ref 282. Copyright 2019 American Chemical Society.

mol^{-1}), CHD (BDE = 77 kcal mol^{-1}), and triphenylmethane (BDE = 81 kcal mol^{-1}). Reaction rates correlate linearly with substrate BDE, and a large KIE (13) was observed upon addition of $[D_2]$-xanthene to **24-Sc**. Although the addition of Lewis acids stabilizes high-valent Co−oxo complex **24-Sc**, HAT to **24** was not reported, so the effect of the Lewis acid cannot firmly be established.

HAT was reported with high-valent cobalt complex $[(TMG_3tren)Co^{IV}(O)Sc(OTf)_3]^{2+}$ (**37-Sc**) in the presence of 9,10-dihydroanthracene.[148] Compared to the corresponding iodosobenzene adduct $[(TMG_3tren)Co^{II}(OI^sPh)]^{2+}$ (**37**), the rate of HAT to **37-Sc** is much slower. Although no explanation was given for the observed rate difference, the nature of the ligand (TMG_3tren) and the presence of Sc^{3+}, might render the reactive Co^{IV}−oxo sterically inaccessible to result in efficient HAT. Nonetheless, further studies are required to determine the mechanism of HAT with **37-Sc**. As previously discussed, other studies have suggested that for **37-Sc** an assignment of $[(TMG_3tren)Co^{III}(OH)Sc(OTf)_3]^{+}$ might be more reasonable, which would significantly alter the driving force and mechanism for HAT by this complex.[162]

The effects of redox-inactive metals on HAT to a series of V^{IV}−oxo complexes were studied.[278] In particular, for $[(TPA)]V^{IV}(O)Cl]$ (**38**) the addition of a variety of redox inactive metals (Na^+, Mg^{2+}, Ca^{2+}, Ba^{2+}, Zn^{2+}, Y^{3+}, Yb^{3+}, Al^{3+}, and Sc^{3+}) greatly accelerated HAT from CHD. During the reaction, formation of the peroxide species $[(TPA)V^{V}(O)(O_2^{2-})]^{+}$ was observed by UV−vis spectroscopy. Interestingly, both Lewis acid and CHD are necessary in order to observe this intermediate. The redox-inactive metal most likely facilitates the dissociation of the chloride ligand from V^{IV}, opening a coordination site on the metal center for binding and subsequent activation of O_2.[278] O_2 activation might also be further enhanced by coordination of the Lewis acid to the V^{IV}−oxo moiety. Upon $1e^-$ oxidation of the metal center, a transiently stable $[(TPA)V^{V}(O)(O_2^{\bullet-})]^{2+}$ species is formed, which abstracts a hydrogen atom from CHD to form $[(TPA)V^{V}(O)(OOH)Cl]^{2+}$. This hydroperoxo species decomposes, possibly via multiple pathways, to regenerate $[(TPA)V^{V}(O)(O_2^{2-})]^{+}$, which is again able to abstract a hydrogen atom from CHD to form $[(TPA)V^{V}(O)(OOH)]^{+}$. The latter HAT process is facilitated by Lewis acids, as in their absence $[(TPA)V^{V}(O)(O_2^{2-})]$ is incapable of undergoing HAT reactions. Unfortunately, no direct correlation between the rate of HAT and the nature of the Lewis acid could be established due to the lack of quantitative rate information in published works, although it appears that the conversion of CHD to benzene qualitatively increases as the Lewis acidity of the redox-inactive metal increases.[278]

These representative examples highlight the importance of redox-inactive metals and their impact on the mechanism of C−H bond cleavage. Whereas Lewis acids typically accelerate the rate of OAT, their effects on C−H bond cleavage are more complex. In systems where concerted H atom abstraction is rate-limiting, rates are often unchanged or even lower in the presence of Lewis acids.[165] In these systems, typically involving substrates with very positive reduction potentials for their $1e^-$ oxidations, large KIEs are observed.[165,276] Decreases in HAT rates can be ascribed to the presence of the redox-inactive metal sterically restricting access to the high-valent metal−oxo moiety.[277] In contrast, rate enhancements are generally observed if a large driving force for ET is present (e.g., for substrates that can be oxidized at sufficiently negative potentials or metal complexes with particularly positive reduction potentials). In these instances, MCET/PCET mechanisms are proposed where ET is the rate-determining step and negligible KIEs are observed.[184,276] The fine balance between these two mechanisms is elegantly demonstrated in the oxidation of benzyl alcohol by complex **17**.[276]

In contrast, ligand design can restrict the Lewis acid from the site of HAT, thereby preventing steric effects from influencing the observed reactivity. Salophen ligands with crown ether moieties discussed previously have been shown to support terminal Mn−nitride complexes (supported by analogous ligands as **1-Mn**, Figure 2).[80,279] Redox-inactive metals bind exclusively at the crown ether site, and modulate the reduction potentials as well as HAT reactivity of this complex. Addition of Lewis acidic metals (Na^+, K^+, Ba^{2+}, Sr^{2+}, La^{3+}, Eu^{3+}) significantly affects both the Mn^{VI}/Mn^{V} reduction potentials (range of >700 mV) and pK_a of the corresponding Mn^{V}−imido complex(by ∼9 pK_a units), with a higher charge cation resulting in lower pKa and higher $E_{1/2}$. This compensatory relationship results in a relatively small change in BDFE, spanning a range of only ∼6 kcal/mol, as constrained by the Bordwell equation.[280] Conceptually related with respect to effects of the charge of remote metal centers, a series of pyrazolate supported $Fe_3MO(OH_x)$ clusters (**39**; M = Mn, Fe) display more significant changes in O−H BDFE (∼16 kcal/mol) upon modulation of charge and oxidation state of the distal iron centers (Figure 9).[281,282] These results highlight

https://doi.org/10.1021/jacsau.3c00675
JACS Au 2024, 4, 344−368

how properties of the entire cluster or bimetallic system, including at distal metal centers, can significantly affect substrate activation and reactivity.

7. CONCLUSIONS

Lewis acidic metal centers can profoundly affect redox processes even without the intrinsic ability to directly participate in electron transfer. Upon coordination to redox active metal complexes, these Lewis acids impact a range of properties, including the reduction potential of transition metal centers, the electrophilicity and nucleophilicity of metal−oxo, −hydroxo, −peroxo, and −superoxo species, and the steric profile of these motifs. Through these effects, redox-inactive metals influence the electron and group transfer reactions of mono- and multimetallic redox-active complexes including the kinetics of ET, OAT, and HAT reactions. These effects can contribute to the enhancement of activity of otherwise unreactive species, prompt shifts in the mechanism of certain transformations, and help direct product selectivity in various chemical reactions. The growing number of examples of these multimetallic effects highlights the general nature of these influences and shows that they can serve as crucial tools to modulate the reactivity of redox-active complexes. Furthermore, many studies have highlighted systematic effects of Lewis acidic metals of potential relevance to biological active sites such as the oxygen-evolving complex and to mixed-metal heterogeneous catalytic systems for water oxidation and O_2 reduction. While many questions about the role played by redox-inactive metals in the actual mechanisms of these complex transformations remain open, the expanding and outstanding studies in this field continue to provide the insights and tools to attempt to answer them.

AUTHOR INFORMATION

Corresponding Author

Theodor Agapie − *Division of Chemistry and Chemical Engineering, California Institute of Technology, Pasadena, California 91125, United States;* orcid.org/0000-0002-9692-7614; Email: agapie@caltech.edu

Authors

Davide Lionetti − *Division of Chemistry and Chemical Engineering, California Institute of Technology, Pasadena, California 91125, United States;* Present Address: Department of Chemistry, Franklin & Marshall College, 415 Harrisburg Avenue, Lancaster, PA 17603

Sandy Suseno − *Division of Chemistry and Chemical Engineering, California Institute of Technology, Pasadena, California 91125, United States*

Angela A. Shiau − *Division of Chemistry and Chemical Engineering, California Institute of Technology, Pasadena, California 91125, United States*

Graham de Ruiter − *Division of Chemistry and Chemical Engineering, California Institute of Technology, Pasadena, California 91125, United States;* orcid.org/0000-0001-6008-286X

Complete contact information is available at: https://pubs.acs.org/10.1021/jacsau.3c00675

Notes

The authors declare no competing financial interest.

ACKNOWLEDGMENTS

T.A. is grateful to the talented students and postdoctoral scholars who have contributed to projects on multimetallic complexes related to protein active sites developed in the Agapie lab, some of which are included in this Perspective, and to collaborators who have studied these compounds and helped understand their properties. T.A. thanks the NIH (R01-GM102687B) and NSF (CHE-1905320) for generously funding research related to bioinorganic chemistry in his laboratory.

REFERENCES

(1) Bertini, G.; Gray, H. B.; Valentine, J. S.; Stiefel, E. I. *Biological Inorganic Chemistry: Structure and Reactivity*; University Science Books, 2007.

(2) Yano, J.; Yachandra, V. Mn4Ca Cluster in Photosynthesis: Where and How Water is Oxidized to Dioxygen. *Chem. Rev.* **2014**, *114* (8), 4175−4205.

(3) Solomon, E. I.; Heppner, D. E.; Johnston, E. M.; Ginsbach, J. W.; Cirera, J.; Qayyum, M.; Kieber-Emmons, M. T.; Kjaergaard, C. H.; Hadt, R. G.; Tian, L. Copper Active Sites in Biology. *Chem. Rev.* **2014**, *114* (7), 3659−3853.

(4) Can, M.; Armstrong, F. A.; Ragsdale, S. W. Structure, Function, and Mechanism of the Nickel Metalloenzymes, CO Dehydrogenase, and Acetyl-CoA Synthase. *Chem. Rev.* **2014**, *114* (8), 4149−4174.

(5) Einsle, O.; Rees, D. C. Structural Enzymology of Nitrogenase Enzymes. *Chem. Rev.* **2020**, *120* (12), 4969−5004.

(6) Lubitz, W.; Ogata, H.; Rüdiger, O.; Reijerse, E. Hydrogenases. *Chem. Rev.* **2014**, *114* (8), 4081−4148.

(7) Schilter, D.; Camara, J. M.; Huynh, M. T.; Hammes-Schiffer, S.; Rauchfuss, T. B. Hydrogenase Enzymes and Their Synthetic Models: The Role of Metal Hydrides. *Chem. Rev.* **2016**, *116* (15), 8693−8749.

(8) Hematian, S.; Garcia-Bosch, I.; Karlin, K. D. Synthetic Heme/Copper Assemblies: Toward an Understanding of Cytochrome c Oxidase Interactions with Dioxygen and Nitrogen Oxides. *Acc. Chem. Res.* **2015**, *48* (8), 2462−2474.

(9) Citek, C.; Herres-Pawlis, S.; Stack, T. D. P. Low Temperature Syntheses and Reactivity of Cu_2O_2 Active-Site Models. *Acc. Chem. Res.* **2015**, *48* (8), 2424−2433.

(10) Fitzpatrick, J.; Kim, E. Synthetic Modeling Chemistry of Iron−Sulfur Clusters in Nitric Oxide Signaling. *Acc. Chem. Res.* **2015**, *48* (8), 2453−2461.

(11) McWilliams, S. F.; Holland, P. L. Dinitrogen Binding and Cleavage by Multinuclear Iron Complexes. *Acc. Chem. Res.* **2015**, *48* (7), 2059−2065.

(12) Serrano-Plana, J.; Garcia-Bosch, I.; Company, A.; Costas, M. Structural and Reactivity Models for Copper Oxygenases: Cooperative Effects and Novel Reactivities. *Acc. Chem. Res.* **2015**, *48* (8), 2397−2406.

(13) Rauchfuss, T. B. Diiron Azadithiolates as Models for the [FeFe]-Hydrogenase Active Site and Paradigm for the Role of the Second Coordination Sphere. *Acc. Chem. Res.* **2015**, *48* (7), 2107−2116.

(14) Lee, S. C.; Lo, W.; Holm, R. H. Developments in the Biomimetic Chemistry of Cubane-Type and Higher Nuclearity Iron−Sulfur Clusters. *Chem. Rev.* **2014**, *114* (7), 3579−3600.

(15) Garcia-Bosch, I.; Ribas, X.; Costas, M. Well-Defined Heterometallic and Unsymmetric M_2O_2 Complexes Arising from Binding and Activation of O_2. *Eur. J. Inorg. Chem.* **2012**, *2012* (2), 179−187.

(16) Tinberg, C. E.; Lippard, S. J. Dioxygen Activation in Soluble Methane Monooxygenase. *Acc. Chem. Res.* **2011**, *44* (4), 280−288.

(17) Friedle, S.; Reisner, E.; Lippard, S. J. Current challenges of modeling diiron enzyme active sites for dioxygen activation by biomimetic synthetic complexes. *Chem. Soc. Rev.* **2010**, *39* (8), 2768−2779.

(18) Gahan, L. R.; Smith, S. J.; Neves, A.; Schenk, G. Phosphate Ester Hydrolysis: Metal Complexes As Purple Acid Phosphatase and Phosphotriesterase Analogues. *Eur. J. Inorg. Chem.* **2009**, *2009* (19), 2745−2758.
(19) Rakowski Dubois, M.; Dubois, D. L. Development of Molecular Electrocatalysts for CO_2 Reduction and H_2 Production/Oxidation. *Acc. Chem. Res.* **2009**, *42* (12), 1974−1982.
(20) Que, L.; Tolman, W. B. Biologically inspired oxidation catalysis. *Nature* **2008**, *455* (7211), 333−340.
(21) Harrop, T. C.; Mascharak, P. K. Structural and spectroscopic models of the A-cluster of acetyl coenzyme a synthase/carbon monoxide dehydrogenase: Nature's Monsanto acetic acid catalyst. *Coord. Chem. Rev.* **2005**, *249* (24), 3007−3024.
(22) Collman, J. P.; Boulatov, R.; Sunderland, C. J.; Fu, L. Functional Analogues of Cytochrome c Oxidase, Myoglobin, and Hemoglobin. *Chem. Rev.* **2004**, *104* (2), 561−588.
(23) Kärkäs, M. D.; Verho, O.; Johnston, E. V.; Åkermark, B. Artificial Photosynthesis: Molecular Systems for Catalytic Water Oxidation. *Chem. Rev.* **2014**, *114* (24), 11863−12001.
(24) Kim, E.; Chufán, E. E.; Kamaraj, K.; Karlin, K. D. Synthetic Models for Heme−Copper Oxidases. *Chem. Rev.* **2004**, *104* (2), 1077−1134.
(25) Tard, C.; Pickett, C. J. Structural and Functional Analogues of the Active Sites of the [Fe]-, [NiFe]-, and [FeFe]-Hydrogenases. *Chem. Rev.* **2009**, *109* (6), 2245−2274.
(26) Holm, R. H.; Lo, W. Structural Conversions of Synthetic and Protein-Bound Iron−Sulfur Clusters. *Chem. Rev.* **2016**, *116* (22), 13685−13713.
(27) Brown, A. C.; Suess, D. L. M. 8.08 - Synthetic Iron-Sulfur Clusters. In *Comprehensive Coordination Chemistry III*; Constable, E. C., Parkin, G., Que, L., Jr., Eds.; Elsevier: Oxford, 2021; pp 134−156.
(28) Tanifuji, K.; Ohki, Y. Metal−Sulfur Compounds in N_2 Reduction and Nitrogenase-Related Chemistry. *Chem. Rev.* **2020**, *120* (12), 5194−5251.
(29) Tainer, J. A.; Getzoff, E. D.; Beem, K. M.; Richardson, J. S.; Richardson, D. C. Determination and Analysis of the 2a Structure of Copper, Zinc Superoxide-Dismutase. *J. Mol. Biol.* **1982**, *160* (2), 181−217.
(30) Pantoliano, M. W.; Valentine, J. S.; Burger, A. R.; Lippard, S. J. A pH-dependent superoxide dismutase activity for zinc-free bovine erythrocuprein. Reexamination of the role of zinc in the holoprotein. *J. Inorg. Biochem.* **1982**, *17* (4), 325−341.
(31) Valentine, J. S.; Mota de Freitas, D. Copper-zinc superoxide dismutase: A unique biological ″ligand″ for bioinorganic studies. *J. Chem. Educ.* **1985**, *62* (11), 990.
(32) Pelmenschikov, V.; Siegbahn, P. E. M. Copper−Zinc Superoxide Dismutase: Theoretical Insights into the Catalytic Mechanism. *Inorg. Chem.* **2005**, *44* (9), 3311−3320.
(33) Tsui, E. Y.; Kanady, J. S.; Agapie, T. Synthetic Cluster Models of Biological and Heterogeneous Manganese Catalysts for O_2 Evolution. *Inorg. Chem.* **2013**, *52* (24), 13833−13848.
(34) Young, K. J.; Brennan, B. J.; Tagore, R.; Brudvig, G. W. Photosynthetic Water Oxidation: Insights from Manganese Model Chemistry. *Acc. Chem. Res.* **2015**, *48* (3), 567−574.
(35) Blakemore, J. D.; Crabtree, R. H.; Brudvig, G. W. Molecular Catalysts for Water Oxidation. *Chem. Rev.* **2015**, *115* (23), 12974−13005.
(36) Najafpour, M. M.; Ehrenberg, T.; Wiechen, M.; Kurz, P. Calcium Manganese(III) Oxides ($CaMn_2O_4{\cdot}x\ H_2O$) as Biomimetic Oxygen-Evolving Catalysts. *Angew. Chem., Int. Ed.* **2010**, *49* (12), 2233−2237.
(37) Wiechen, M.; Zaharieva, I.; Dau, H.; Kurz, P. Layered manganese oxides for water-oxidation: alkaline earth cations influence catalytic activity in a photosystem II-like fashion. *Chem. Sci.* **2012**, *3* (7), 2330−2339.
(38) Najafpour, M. M.; Isaloo, M. A.; Ghobadi, M. Z.; Amini, E.; Haghighi, B. The effect of different metal ions between nanolayers of manganese oxide on water oxidation. *Journal of Photochemistry and Photobiology B: Biology* **2014**, *141*, 247−252.
(39) Zaharieva, I.; Najafpour, M. M.; Wiechen, M.; Haumann, M.; Kurz, P.; Dau, H. Synthetic manganese-calcium oxides mimic the water-oxidizing complex of photosynthesis functionally and structurally. *Energy Environ. Sci.* **2011**, *4* (7), 2400−2408.
(40) Najafpour, M. M.; Isaloo, M. A.; Hołyńska, M.; Shen, J.-R.; Allakhverdiev, S. The effect of lanthanum(III) and cerium(III) ions between layers of manganese oxide on water oxidation. *Photosynth. Res.* **2015**, *126* (2), 489−498.
(41) Park, J.; Hong, S. Cooperative bimetallic catalysis in asymmetric transformations. *Chem. Soc. Rev.* **2012**, *41* (21), 6931−6943.
(42) Buchwalter, P.; Rosé, J.; Braunstein, P. Multimetallic Catalysis Based on Heterometallic Complexes and Clusters. *Chem. Rev.* **2015**, *115* (1), 28−126.
(43) Cooper, B. G.; Napoline, J. W.; Thomas, C. M. Catalytic Applications of Early/Late Heterobimetallic Complexes. *Catalysis Reviews* **2012**, *54* (1), 1−40.
(44) Braunstein, P.; Rosé, J. Heterometallic Clusters in Catalysis. In *Metal Clusters in Chemistry*; Wiley-VCH Verlag GmbH: 2008; pp 616−677.
(45) Powers, I. G.; Uyeda, C. Metal-Metal Bonds in Catalysis. *ACS Catal.* **2017**, *7* (2), 936−958.
(46) Pye, D. R.; Mankad, N. P. Bimetallic catalysis for C-C and C-X coupling reactions. *Chem. Sci.* **2017**, *8* (3), 1705−1718.
(47) Corma, A.; García, H. Lewis Acids: From Conventional Homogeneous to Green Homogeneous and Heterogeneous Catalysis. *Chem. Rev.* **2003**, *103* (11), 4307−4366.
(48) Corma, A.; García, H. Lewis Acids as Catalysts in Oxidation Reactions: From Homogeneous to Heterogeneous Systems. *Chem. Rev.* **2002**, *102* (10), 3837−3892.
(49) Fukuzumi, S. Roles of Metal Ions in Controlling Bioinspired Electron-Transfer Systems. Metal Ion-Coupled Electron Transfer. In *Progress in Inorganic Chemistry*; John Wiley & Sons, Inc.: 2009; pp 49−154.
(50) Fukuzumi, S.; Ohkubo, K. Metal ion-coupled and decoupled electron transfer. *Coord. Chem. Rev.* **2010**, *254* (3−4), 372−385.
(51) Fukuzumi, S. Catalytic control of electron-transfer processes. *Pure Appl. Chem.* **2003**, *75*, 577.
(52) Fukuzumi, S.; Jung, J.; Lee, Y.-M.; Nam, W. Effects of Lewis Acids on Photoredox Catalysis. *Asian Journal of Organic Chemistry* **2017**, *6* (4), 397−409.
(53) Connor, G. P.; Holland, P. L. Coordination chemistry insights into the role of alkali metal promoters in dinitrogen reduction. *Catal. Today* **2017**, *286*, 21−40.
(54) Liu, Y.; Lau, T.-C. Activation of Metal Oxo and Nitrido Complexes by Lewis Acids. *J. Am. Chem. Soc.* **2019**, *141* (9), 3755−3766.
(55) Devi, T.; Lee, Y.-M.; Nam, W.; Fukuzumi, S. Metal ion-coupled electron-transfer reactions of metal-oxygen complexes. *Coord. Chem. Rev.* **2020**, *410*, No. 213219.
(56) Kumar, A.; Blakemore, J. D. On the Use of Aqueous Metal-Aqua pK_a Values as a Descriptor of Lewis Acidity. *Inorg. Chem.* **2021**, *60* (2), 1107−1115.
(57) Golwankar, R. R.; Curry, T. D., II; Paranjothi, C. J.; Blakemore, J. D. Molecular Influences on the Quantification of Lewis Acidity with Phosphine Oxide Probes. *Inorg. Chem.* **2023**, *62* (25), 9765−9780.
(58) Beckett, M. A.; Strickland, G. C.; Holland, J. R.; Sukumar Varma, K. A convenient n.m.r. method for the measurement of Lewis acidity at boron centres: correlation of reaction rates of Lewis acid initiated epoxide polymerizations with Lewis acidity. *Polymer* **1996**, *37* (20), 4629−4631.
(59) Mayer, U.; Gutmann, V.; Gerger, W. The acceptor number — A quantitative empirical parameter for the electrophilic properties of solvents. *Monatshefte für Chemie/Chemical Monthly* **1975**, *106* (6), 1235−1257.
(60) Gaffen, J. R.; Bentley, J. N.; Torres, L. C.; Chu, C.; Baumgartner, T.; Caputo, C. B. A Simple and Effective Method of Determining Lewis Acidity by Using Fluorescence. *Chem.* **2019**, *5* (6), 1567−1583.

https://doi.org/10.1021/jacsau.3c00675
JACS Au 2024, 4, 344−368

(61) Bentley, J. N.; Elgadi, S. A.; Gaffen, J. R.; Demay-Drouhard, P.; Baumgartner, T.; Caputo, C. B. Fluorescent Lewis Adducts: A Practical Guide to Relative Lewis Acidity. *Organometallics* **2020**, *39* (20), 3645−3655.
(62) Fukuzumi, S.; Ohkubo, K. Quantitative Evaluation of Lewis Acidity of Metal Ions Derived from the g Values of ESR Spectra of Superoxide: Metal Ion Complexes in Relation to the Promoting Effects in Electron Transfer Reactions. *Chem.—Eur. J.* **2000**, *6* (24), 4532−4535.
(63) Perrin, D. D. *Ionisation Constants of Inorganic Acids and Bases in Aqueous Solution*; Elsevier, 1982.
(64) Hawkes, S. J. All Positive Ions Give Acid Solutions in Water. *J. Chem. Educ.* **1996**, *73* (6), 516.
(65) *CRC Handbook of Chemistry and Physics*, 104th ed.; CRC Press/Taylor & Francis, 2023.
(66) Speight, J. G. *Lange's Handbook of Chemistry*, 16th ed.; McGraw-Hill Education: New York, 2005.
(67) Krewald, V.; Neese, F.; Pantazis, D. A. Redox potential tuning by redox-inactive cations in nature's water oxidizing catalyst and synthetic analogues. *Phys. Chem. Chem. Phys.* **2016**, *18* (16), 10739−10750.
(68) Reath, A. H.; Ziller, J. W.; Tsay, C.; Ryan, A. J.; Yang, J. Y. Redox Potential and Electronic Structure Effects of Proximal Nonredox Active Cations in Cobalt Schiff Base Complexes. *Inorg. Chem.* **2017**, *56* (6), 3713−3718.
(69) Plenio, H.; Diodone, R. Complexation of Na^+ in redox-active ferrocene crown ethers, a structural investigation, and an unexpected case of Li^+ selectivity. *Inorg. Chem.* **1995**, *34* (15), 3964−3972.
(70) Horwitz, C. P.; Warden, J. T.; Weintraub, S. T. Electron spin resonance and electrospray ionization mass spectroscopic studies of the interaction of alkali and alkaline earth cations with manganese bis(μ-oxo) dimers. *Inorg. Chim. Acta* **1996**, *246* (1), 311−320.
(71) Horwitz, C. P.; Ciringh, Y.; Weintraub, S. T. Formation pathway of a Mn(IV),Mn(IV) bis(μ-oxo) dimer that incorporates alkali and alkaline earth cations and electron transfer properties of the dimer. *Inorg. Chim. Acta* **1999**, *294* (2), 133−139.
(72) Horwitz, C. P.; Ciringh, Y. Synthesis and electrochemical properties of oxo-bridged manganese dimers incorporating alkali and alkaline earth cations. *Inorg. Chim. Acta* **1994**, *225* (1−2), 191−200.
(73) Delgado, M.; Ziegler, J. M.; Seda, T.; Zakharov, L. N.; Gilbertson, J. D. Pyridinediimine iron complexes with pendant redox-inactive metals located in the secondary coordination sphere. *Inorg. Chem.* **2016**, *55* (2), 555−557.
(74) Beer, P. D.; Blackburn, C.; McAleer, J. F.; Sikanyika, H. Redox-responsive crown ethers containing a conjugated link between the ferrocene moiety and a benzo crown ether. *Inorg. Chem.* **1990**, *29* (3), 378−381.
(75) Andrews, M. P.; Blackburn, C.; McAleer, J. F.; Patel, V. D. Redox-active crown ethers: transmission of cation binding to a redox centre via a conjugated link. *J. Chem. Soc., Chem. Commun.* **1987**, No. 14, 1122−1124.
(76) Al Obaidi, N.; Beer, P. D.; Bright, J. P.; Jones, C. J.; McCleverty, J. A.; Salam, S. S. The synthesis and electrochemistry of novel redox responsive molybdenum complexes containing cyclic polyether cation binding sites. *J. Chem. Soc., Chem. Commun.* **1986**, No. 3, 239−241.
(77) Kumar, A.; Lionetti, D.; Day, V. W.; Blakemore, J. D. Redox-Inactive Metal Cations Modulate the Reduction Potential of the Uranyl Ion in Macrocyclic Complexes. *J. Am. Chem. Soc.* **2020**, *142* (6), 3032−3041.
(78) Kumar, A.; Lionetti, D.; Day, V. W.; Blakemore, J. D. Trivalent Lewis Acidic Cations Govern the Electronic Properties and Stability of Heterobimetallic Complexes of Nickel. *Chem.—Eur. J.* **2018**, *24* (1), 141−149.
(79) Barlow, J. M.; Ziller, J. W.; Yang, J. Y. Inhibiting the Hydrogen Evolution Reaction (HER) with Proximal Cations: A Strategy for Promoting Selective Electrocatalytic Reduction. *ACS Catal.* **2021**, *11* (13), 8155−8164.
(80) Chantarojsiri, T.; Reath, A. H.; Yang, J. Y. Cationic Charges Leading to an Inverse Free-Energy Relationship for N−N Bond Formation by Mn^{VI} Nitrides. *Angew. Chem., Int. Ed.* **2018**, *57* (43), 14037−14042.
(81) Chantarojsiri, T.; Ziller, J. W.; Yang, J. Y. Incorporation of redox-inactive cations promotes iron catalyzed aerobic C−H oxidation at mild potentials. *Chem. Sci.* **2018**, *9* (9), 2567−2574.
(82) Idris, N. S.; Barlow, J. M.; Chabolla, S. A.; Ziller, J. W.; Yang, J. Y. Synthesis and redox properties of heterobimetallic Re($bpy^{Crown\text{-}M}$)-$(CO)_3Cl$ complexes, where M = Na^+, K^+, Ca^{2+}, and Ba^{2+}. *Polyhedron* **2021**, *208*, No. 115385.
(83) Kang, K.; Fuller, J.; Reath, A. H.; Ziller, J. W.; Alexandrova, A. N.; Yang, J. Y. Installation of internal electric fields by non-redox active cations in transition metal complexes. *Chem. Sci.* **2019**, *10* (43), 10135−10142.
(84) Golwankar, R. R.; Kumar, A.; Day, V. W.; Blakemore, J. D. Revealing the Influence of Diverse Secondary Metal Cations on Redox-Active Palladium Complexes. *Chem.—Eur. J.* **2022**, *28* (38), No. e202200344.
(85) Kelsey, S. R.; Kumar, A.; Oliver, A. G.; Day, V. W.; Blakemore, J. D. Promotion and Tuning of the Electrochemical Reduction of Hetero- and Homobimetallic Zinc Complexes. *ChemElectroChem.* **2021**, *8* (15), 2792−2802.
(86) Nguyen, H. M.; Morgan, H. W. T.; Chantarojsiri, T.; Kerr, T. A.; Yang, J. Y.; Alexandrova, A. N.; Léonard, N. G. Charge and Solvent Effects on the Redox Behavior of Vanadyl Salen−Crown Complexes. *J. Phys. Chem. A* **2023**, *127* (25), 5324−5334.
(87) Dopp, C. M.; Golwankar, R. R.; Kelsey, S. R.; Douglas, J. T.; Erickson, A. N.; Oliver, A. G.; Day, C. S.; Day, V. W.; Blakemore, J. D. Vanadyl as a Spectroscopic Probe of Tunable Ligand Donor Strength in Bimetallic Complexes. *Inorg. Chem.* **2023**, *62* (25), 9827−9843.
(88) Teptarakulkarn, P.; Lorpaiboon, W.; Anusanti, T.; Laowiwatkasem, N.; Chainok, K.; Sangtrirutnugul, P.; Surawatanawong, P.; Chantarojsiri, T. Incorporation of Cation Affects the Redox Reactivity of Fe−NNN Complexes on C−H Oxidation. *Inorg. Chem.* **2022**, *61* (29), 11066−11074.
(89) Akine, S. Novel ion recognition systems based on cyclic and acyclic oligo(salen)-type ligands. *J. Inclusion Phenom. Macrocyclic Chem.* **2012**, *72* (1), 25−54.
(90) Batista, S. C.; Neves, A.; Bortoluzzi, A. J.; Vencato, I.; Peralta, R. A.; Szpoganicz, B.; Aires, V. V. E.; Terenzi, H.; Severino, P. C. Highly efficient phosphate diester hydrolysis and DNA interaction by a new unsymmetrical $Fe^{III}Ni^{II}$ model complex. *Inorg. Chem. Commun.* **2003**, *6* (8), 1161−1165.
(91) Fraser, C.; Bosnich, B. Bimetallic reactivity - investigation of metal-metal interaction in complexes of a chiral macrocyclic binucleating ligand bearing 6-coordinate and 4-coordinate sites. *Inorg. Chem.* **1994**, *33* (2), 338−346.
(92) Fraser, C.; Johnston, L.; Rheingold, A. L.; Haggerty, B. S.; Williams, G. K.; Whelan, J.; Bosnich, B. Bimetallic reactivity - synthesis, structure, and reactivity of homobimetallic and heterobimetallic complexes of a binucleating macrocyclic ligand containing 6-coordination and 4-coordination sites. *Inorg. Chem.* **1992**, *31* (10), 1835−1844.
(93) Fraser, C.; Ostrander, R.; Rheingold, A. L.; White, C.; Bosnich, B. Bimetallic reactivity - controlled synthesis of monometallic and homo-bimetallic and heterobimetallic complexes of a chiral binucleating macrocyclic ligand bearing 6- and 4-coordinate sites. *Inorg. Chem.* **1994**, *33* (2), 324−337.
(94) Ghiladi, M.; McKenzie, C. J.; Meier, A.; Powell, A. K.; Ulstrup, J.; Wocadlo, S. Dinuclear iron(III)-metal(II) complexes as structural core models for purple acid phosphatases. *J. Chem. Soc. Dalton* **1997**, No. 21, 4011−4018.
(95) Karsten, P.; Neves, A.; Bortoluzzi, A. J.; Lanznaster, M.; Drago, V. Synthesis, structure, properties, and phosphatase-like activity of the first heterodinuclear $FeMn^{II}$ complex with the unsymmetric ligand H_2BPBPMP as a model for the PAP in sweet potato. *Inorg. Chem.* **2002**, *41* (18), 4624−4626.

https://doi.org/10.1021/jacsau.3c00675
JACS Au 2024, 4, 344−368

(96) Lanznaster, M.; Neves, A.; Bortoluzzi, A. J.; Szpoganicz, B.; Schwingel, E. New $Fe^{III}Zn^{II}$ complex containing a single terminal Fe−$O_{phenolate}$ bond as a structural and functional model for the active site of red kidney bean purple acid phosphatase. *Inorg. Chem.* **2002**, *41*, 5641−5643.
(97) McCollum, D. G.; Fraser, C.; Ostrander, R.; Rheingold, A. L.; Bosnich, B. Bimetallic reactivity - general-synthesis of binucleating macrocyclic ligands containing 6-coordinate and 4-coordinate sites. *Inorg. Chem.* **1994**, *33* (11), 2383−2392.
(98) McCollum, D. G.; Hall, L.; White, C.; Ostrander, R.; Rheingold, A. L.; Whelan, J.; Bosnich, B. Bimetallic reactivity - preparation and characterization of symmetrical bimetallic complexes of a binucleating macrocyclic ligand, cytim, containing 6-coordinate and 4-coordinate sites. *Inorg. Chem.* **1994**, *33* (5), 924−933.
(99) McCollum, D. G.; Yap, G. P. A.; LiableSands, L.; Rheingold, A. L.; Bosnich, B. Bimetallic reactivity. Oxo transfer reactions with a heterobimetallic complex of Iron(II) and Vanadium(III). *Inorg. Chem.* **1997**, *36* (10), 2230.
(100) McCollum, D. G.; Yap, G. P. A.; Rheingold, A. L.; Bosnich, B. Bimetallic reactivity. Synthesis of bimetallic complexes of macrocyclic binucleating ligands containing 6- and 4-coordinate sites and their reactivity with dioxygen and other oxidants. *J. Am. Chem. Soc.* **1996**, *118* (6), 1365−1379.
(101) Schenk, G.; Peralta, R. A.; Batista, S. C.; Bortoluzzi, A. J.; Szpoganicz, B.; Dick, A. K.; Herrald, P.; Hanson, G. R.; Szilagyi, R. K.; Riley, M. J.; Gahan, L. R.; Neves, A. Probing the role of the divalent metal ion in uteroferrin using metal ion replacement and a comparison to isostructural biomimetics. *J. Biol. Inorg. Chem.* **2007**, *13* (1), 139−155.
(102) Xavier, F. R.; Neves, A.; Casellato, A.; Peralta, R. A.; Bortoluzzi, A. J.; Szpoganicz, B.; Severino, P. C.; Terenzi, H.; Tomkowicz, Z.; Ostrovsky, S.; Haase, W.; Ozarowski, A.; Krzystek, J.; Telser, J.; Schenk, G.; Gahan, L. R. Unsymmetrical $FeCo^{II}$ and $GaCo^{II}$ complexes as chemical hydrolases: Biomimetic models for purple acid phosphatases (paps). *Inorg. Chem.* **2009**, *48* (16), 7905−7921.
(103) Ghosh, T. K.; Maity, S.; Ghosh, S.; Gomila, R. M.; Frontera, A.; Ghosh, A. Role of Redox-Inactive Metal Ions in Modulating the Reduction Potential of Uranyl Schiff Base Complexes: Detailed Experimental and Theoretical Studies. *Inorg. Chem.* **2022**, *61* (18), 7130−7142.
(104) Robinson, J. R.; Gordon, Z.; Booth, C. H.; Carroll, P. J.; Walsh, P. J.; Schelter, E. J. Tuning reactivity and electronic properties through ligand reorganization within a cerium heterobimetallic framework. *J. Am. Chem. Soc.* **2013**, *135* (50), 19016−19024.
(105) Robinson, J. R.; Carroll, P. J.; Walsh, P. J.; Schelter, E. J. The Impact of Ligand Reorganization on Cerium(III) Oxidation Chemistry. *Angew. Chem., Int. Ed.* **2012**, *51* (40), 10159−10163.
(106) Levin, J. R.; Dorfner, W. L.; Carroll, P. J.; Schelter, E. J. Control of cerium oxidation state through metal complex secondary structures. *Chem. Sci.* **2015**, *6* (12), 6925−6934.
(107) Tsui, E. Y.; Tran, R.; Yano, J.; Agapie, T. Redox-inactive metals modulate the reduction potential in heterometallic manganese-oxido clusters. *Nat. Chem.* **2013**, *5* (4), 293−299.
(108) Tsui, E. Y.; Agapie, T. Reduction potentials of heterometallic manganese-oxido cubane complexes modulated by redox-inactive metals. *Proc. Natl. Acad. Sci. U. S. A.* **2013**, *110* (25), 10084−10088.
(109) Lin, P.-H.; Takase, M. K.; Agapie, T. Investigations of the effect of the non-manganese metal in heterometallic-oxido cluster models of the oxygen evolving complex of photosystem II: lanthanides as substitutes for calcium. *Inorg. Chem.* **2015**, *54* (1), 59−64.
(110) Herbert, D. E.; Lionetti, D.; Rittle, J.; Agapie, T. Heterometallic triiron-oxo/hydroxo clusters: effect of redox-inactive metals. *J. Am. Chem. Soc.* **2013**, *135* (51), 19075−19078.
(111) Lionetti, D.; Suseno, S.; Tsui, E. Y.; Lu, L.; Stich, T. A.; Carsch, K. M.; Nielsen, R. J.; Goddard, W. A.; Britt, R. D.; Agapie, T. Effects of Lewis Acidic Metal Ions (M) on Oxygen-Atom Transfer Reactivity of Heterometallic Mn_3MO_4 Cubane and $Fe_3MO(OH)$ and $Mn_3MO(OH)$ Clusters. *Inorg. Chem.* **2019**, *58* (4), 2336−2345.
(112) Kanady, J. S.; Lin, P.-H.; Carsch, K. M.; Nielsen, R. J.; Takase, M. K.; Goddard, W. A.; Agapie, T. Toward Models for the Full Oxygen-Evolving Complex of Photosystem II by Ligand Coordination to Lower the Symmetry of the Mn_3CaO_4 Cubane: Demonstration that Electronic Effects Facilitate Binding of a Fifth Metal. *J. Am. Chem. Soc.* **2014**, *136* (41), 14373−14376.
(113) Zhang, C.; Chen, C.; Dong, H.; Shen, J.-R.; Dau, H.; Zhao, J. A synthetic Mn_4Ca-cluster mimicking the oxygen-evolving center of photosynthesis. *Science* **2015**, *348* (6235), 690−693.
(114) Kanady, J. S.; Tsui, E. Y.; Day, M. W.; Agapie, T. A synthetic model of the Mn_3Ca subsite of the oxygen-evolving complex in photosystem II. *Science* **2011**, *333* (6043), 733−736.
(115) Mukherjee, S.; Stull, J. A.; Yano, J.; Stamatatos, T. C.; Pringouri, K.; Stich, T. A.; Abboud, K. A.; Britt, R. D.; Yachandra, V. K.; Christou, G. Synthetic model of the asymmetric $[Mn_3CaO_4]$ cubane core of the oxygen-evolving complex of photosystem II. *Proc. Natl. Acad. Sci. U. S. A.* **2012**, *109* (7), 2257−2262.
(116) Chen, C.; Chen, Y.; Yao, R.; Li, Y.; Zhang, C. Artificial Mn4Ca Clusters with Exchangeable Solvent Molecules Mimicking the Oxygen-Evolving Center in Photosynthesis. *Angew. Chem., Int. Ed.* **2019**, *58* (12), 3939−3942.
(117) Davis, K. M.; Pushkar, Y. N. Structure of the Oxygen Evolving Complex of Photosystem II at Room Temperature. *J. Phys. Chem. B* **2015**, *119* (8), 3492−3498.
(118) Lohmiller, T.; Shelby, M. L.; Long, X.; Yachandra, V. K.; Yano, J. Removal of Ca^{2+} from the Oxygen-Evolving Complex in Photosystem II Has Minimal Effect on the Mn_4O_5 Core Structure: A Polarized Mn X-ray Absorption Spectroscopy Study. *J. Phys. Chem. B* **2015**, *119* (43), 13742−13754.
(119) Lee, H. B.; Agapie, T. Redox Tuning via Ligand-Induced Geometric Distortions at a YMn_3O_4 Cubane Model of the Biological Oxygen Evolving Complex. *Inorg. Chem.* **2019**, *58* (22), 14998−15003.
(120) Amtawong, J.; Balcells, D.; Wilcoxen, J.; Handford, R. C.; Biggins, N.; Nguyen, A. I.; Britt, R. D.; Tilley, T. D. Isolation and Study of Ruthenium−Cobalt Oxo Cubanes Bearing a High-Valent, Terminal Ru^{V}−Oxo with Significant Oxyl Radical Character. *J. Am. Chem. Soc.* **2019**, *141* (50), 19859−19869.
(121) Nguyen, A. I.; Wang, J.; Levine, D. S.; Ziegler, M. S.; Tilley, T. D. Synthetic control and empirical prediction of redox potentials for Co_4O_4 cubanes over a 1.4 V range: implications for catalyst design and evaluation of high-valent intermediates in water oxidation. *Chem. Sci.* **2017**, *8* (6), 4274−4284.
(122) Park, Y. J.; Cook, S. A.; Sickerman, N. S.; Sano, Y.; Ziller, J. W.; Borovik, A. S. Heterobimetallic complexes with M^{III}-(μ-OH)-M^{II} cores (M^{III} = Fe, Mn, Ga; M^{II} = Ca, Sr, and Ba): structural, kinetic, and redox properties. *Chem. Sci.* **2013**, *4* (2), 717−726.
(123) Park, Y. J.; Ziller, J. W.; Borovik, A. S. The Effects of Redox-Inactive Metal Ions on the Activation of Dioxygen: Isolation and Characterization of a Heterobimetallic Complex Containing a Mn^{III}−(μ-OH)−Ca^{II} Core. *J. Am. Chem. Soc.* **2011**, *133* (24), 9258−9261.
(124) Oswald, V. F.; Lee, J. L.; Biswas, S.; Weitz, A. C.; Mittra, K.; Fan, R.; Li, J.; Zhao, J.; Hu, M. Y.; Alp, E. E.; Bominaar, E. L.; Guo, Y.; Green, M. T.; Hendrich, M. P.; Borovik, A. S. Effects of Noncovalent Interactions on High-Spin Fe(IV)−Oxido Complexes. *J. Am. Chem. Soc.* **2020**, *142* (27), 11804−11817.
(125) Price, J. C.; Barr, E. W.; Tirupati, B.; Bollinger, J. M.; Krebs, C. The First Direct Characterization of a High-Valent Iron Intermediate in the Reaction of an α-Ketoglutarate-Dependent Dioxygenase: A High-Spin Fe(IV) Complex in Taurine/α-Ketoglutarate Dioxygenase (TauD) from Escherichia coli. *Biochemistry* **2003**, *42* (24), 7497−7508.
(126) Rittle, J.; Green, M. T. Cytochrome P450 Compound I: Capture, Characterization, and C-H Bond Activation Kinetics. *Science* **2010**, *330* (6006), 933−937.
(127) McDonald, A. R.; Que, L., Jr High-valent nonheme iron-oxo complexes: Synthesis, structure, and spectroscopy. *Coord. Chem. Rev.* **2013**, *257* (2), 414−428.

https://doi.org/10.1021/jacsau.3c00675
JACS Au 2024, 4, 344−368

(128) Krebs, C.; Galonić Fujimori, D.; Walsh, C. T.; Bollinger, J. M. Non-Heme Fe(IV)−Oxo Intermediates. *Acc. Chem. Res.* **2007**, *40* (7), 484−492.
(129) Costas, M.; Mehn, M. P.; Jensen, M. P.; Que, L. Dioxygen Activation at Mononuclear Nonheme Iron Active Sites: Enzymes, Models, and Intermediates. *Chem. Rev.* **2004**, *104* (2), 939−986.
(130) Poulos, T. L. Heme Enzyme Structure and Function. *Chem. Rev.* **2014**, *114* (7), 3919−3962.
(131) Feig, A. L.; Lippard, S. J. Reactions of Non-Heme Iron(II) Centers with Dioxygen in Biology and Chemistry. *Chem. Rev.* **1994**, *94* (3), 759−805.
(132) Barber, J. A Mechanism for Water Splitting and Oxygen Production in Photosynthesis. *Nature Plants* **2017**, *3*, No. 17041.
(133) Abu-Omar, M. M. High-valent iron and manganese complexes of corrole and porphyrin in atom transfer and dioxygen evolving catalysis. *Dalton Trans.* **2011**, *40* (14), 3435−3444.
(134) Borovik, A. S. Role of metal-oxo complexes in the cleavage of C-H bonds. *Chem. Soc. Rev.* **2011**, *40* (4), 1870−1874.
(135) Boucher, L. J. Manganese porphyrin complexes. *Coord. Chem. Rev.* **1972**, *7* (3), 289−329.
(136) Hohenberger, J.; Ray, K.; Meyer, K. The biology and chemistry of high-valent iron-oxo and iron-nitrido complexes. *Nat. Commun.* **2012**, *3*, 720.
(137) Liu, W.; Groves, J. T. Manganese Catalyzed C-H Halogenation. *Acc. Chem. Res.* **2015**, *48* (6), 1727−1735.
(138) Meunier, B. Metalloporphyrins as versatile catalysts for oxidation reactions and oxidative DNA cleavage. *Chem. Rev.* **1992**, *92* (6), 1411−1456.
(139) Nam, W. High-Valent Iron(IV)−Oxo Complexes of Heme and Non-Heme Ligands in Oxygenation Reactions. *Acc. Chem. Res.* **2007**, *40* (7), 522−531.
(140) Nam, W. Synthetic Mononuclear Nonheme Iron−Oxygen Intermediates. *Acc. Chem. Res.* **2015**, *48* (8), 2415−2423.
(141) Oszajca, M.; Franke, A.; Brindell, M.; Stochel, G.; van Eldik, R. Redox cycling in the activation of peroxides by iron porphyrin and manganese complexes. 'Catching' catalytic active intermediates. *Coord. Chem. Rev.* **2016**, *306*, 483−509.
(142) Pecoraro, V. L.; Baldwin, M. J.; Gelasco, A. Interaction of Manganese with Dioxygen and Its Reduced Derivatives. *Chem. Rev. (Washington, D. C.)* **1994**, *94* (3), 807−26.
(143) Puri, M.; Que, L. Toward the Synthesis of More Reactive S = 2 Non-Heme Oxoiron(IV) Complexes. *Acc. Chem. Res.* **2015**, *48* (8), 2443−2452.
(144) Que, L. The Road to Non-Heme Oxoferryls and Beyond. *Acc. Chem. Res.* **2007**, *40* (7), 493−500.
(145) Simões, M. M. Q.; Neves, C. M. B.; Pires, S. M. G.; Neves, M. G. P. M. S.; Cavaleiro, J. A. S. Mimicking P450 processes and the use of metalloporphyrins. *Pure Appl. Chem.* **2013**, *85* (8), 1671−1681.
(146) Yoon, H.; Lee, Y.-M.; Wu, X.; Cho, K.-B.; Sarangi, R.; Nam, W.; Fukuzumi, S. Enhanced Electron-Transfer Reactivity of Nonheme Manganese(IV)−Oxo Complexes by Binding Scandium Ions. *J. Am. Chem. Soc.* **2013**, *135* (24), 9186−9194.
(147) Yoon, H.; Lee, Y.-M.; Nam, W.; Fukuzumi, S. Hydride transfer from NADH analogues to a nonheme manganese(IV)-oxo complex via rate-determining electron transfer. *Chem. Commun.* **2014**, *50* (85), 12944−12946.
(148) Pfaff, F. F.; Kundu, S.; Risch, M.; Pandian, S.; Heims, F.; Pryjomska-Ray, I.; Haack, P.; Metzinger, R.; Bill, E.; Dau, H.; Comba, P.; Ray, K. An Oxocobalt(IV) Complex Stabilized by Lewis Acid Interactions with Scandium(III) Ions. *Angew. Chem., Int. Ed.* **2011**, *50* (7), 1711−1715.
(149) Morimoto, Y.; Kotani, H.; Park, J.; Lee, Y.-M.; Nam, W.; Fukuzumi, S. Metal ion-coupled electron transfer of a nonheme oxoiron(IV) complex: remarkable enhancement of electron-transfer rates by Sc^{3+}. *J. Am. Chem. Soc.* **2011**, *133* (3), 403−405.
(150) Leeladee, P.; Baglia, R. A.; Prokop, K. A.; Latifi, R.; de Visser, S. P.; Goldberg, D. P. Valence tautomerism in a high-valent manganese−oxo porphyrinoid complex induced by a Lewis acid. *J. Am. Chem. Soc.* **2012**, *134* (25), 10397−10400.
(151) Hong, S.; Pfaff, F. F.; Kwon, E.; Wang, Y.; Seo, M.-S.; Bill, E.; Ray, K.; Nam, W. Spectroscopic Capture and Reactivity of a Low-Spin Cobalt(IV)-Oxo Complex Stabilized by Binding Redox-Inactive Metal Ions. *Angew. Chem., Int. Ed.* **2014**, *53* (39), 10403−10407.
(152) Hong, S.; Lee, Y.-M.; Sankaralingam, M.; Vardhaman, A. K.; Park, Y. J.; Cho, K.-B.; Ogura, T.; Sarangi, R.; Fukuzumi, S.; Nam, W. A Manganese(V)−Oxo Complex: Synthesis by Dioxygen Activation and Enhancement of Its Oxidizing Power by Binding Scandium Ion. *J. Am. Chem. Soc.* **2016**, *138* (27), 8523−8532.
(153) Fukuzumi, S.; Ohkubo, K.; Lee, Y.-M.; Nam, W. Lewis acid coupled electron transfer of metal−oxygen intermediates. *Chem.—Eur. J.* **2015**, *21* (49), 17548−17559.
(154) Fukuzumi, S.; Morimoto, Y.; Kotani, H.; Naumov, P.; Lee, Y.-M.; Nam, W. Crystal structure of a metal ion-bound oxoiron(IV) complex and implications for biological electron transfer. *Nat. Chem.* **2010**, *2* (9), 756−759.
(155) Rohde, J.-U.; In, J.-H.; Lim, M. H.; Brennessel, W. W.; Bukowski, M. R.; Stubna, A.; Münck, E.; Nam, W.; Que, L. Crystallographic and Spectroscopic Characterization of a Nonheme Fe(IV)═O Complex. *Science* **2003**, *299* (5609), 1037−1039.
(156) Lee, Y.-M.; Kotani, H.; Suenobu, T.; Nam, W.; Fukuzumi, S. Fundamental Electron-Transfer Properties of Non-heme Oxoiron(IV) Complexes. *J. Am. Chem. Soc.* **2008**, *130* (2), 434−435.
(157) Swart, M. A change in the oxidation state of iron: scandium is not innocent. *Chem. Commun.* **2013**, *49* (59), 6650−6652.
(158) Prakash, J.; Rohde, G. T.; Meier, K. K.; Jasniewski, A. J.; Van Heuvelen, K. M.; Münck, E.; Que, L. Spectroscopic Identification of an Fe^{III} Center, not Fe^{IV}, in the Crystalline Sc−O−Fe Adduct Derived from $[Fe^{IV}(O)(TMC)]^{2+}$. *J. Am. Chem. Soc.* **2015**, *137* (10), 3478−3481.
(159) Sankaralingam, M.; Lee, Y.-M.; Pineda-Galvan, Y.; Karmalkar, D. G.; Seo, M. S.; Jeon, S. H.; Pushkar, Y.; Fukuzumi, S.; Nam, W. Redox Reactivity of a Mononuclear Manganese-Oxo Complex Binding Calcium Ion and Other Redox-Inactive Metal Ions. *J. Am. Chem. Soc.* **2019**, *141* (3), 1324−1336.
(160) Devi, T.; Lee, Y.-M.; Nam, W.; Fukuzumi, S. Tuning Electron-Transfer Reactivity of a Chromium(III)−Superoxo Complex Enabled by Calcium Ion and Other Redox-Inactive Metal Ions. *J. Am. Chem. Soc.* **2020**, *142* (1), 365−372.
(161) Barats-Damatov, D.; Shimon, L. J. W.; Weiner, L.; Schreiber, R. E.; Jiménez-Lozano, P.; Poblet, J. M.; de Graaf, C.; Neumann, R. Dicobalt-μ-oxo Polyoxometalate Compound, $[(\alpha_2\text{-}P_2W_{17}O_{61}Co)_2O]^{14-}$: A Potent Species for Water Oxidation, C−H Bond Activation, and Oxygen Transfer. *Inorg. Chem.* **2014**, *53* (3), 1779−1787.
(162) Lacy, D. C.; Park, Y. J.; Ziller, J. W.; Yano, J.; Borovik, A. S. Assembly and Properties of Heterobimetallic $Co^{II/III}/Ca^{II}$ Complexes with Aquo and Hydroxo Ligands. *J. Am. Chem. Soc.* **2012**, *134* (42), 17526−17535.
(163) Fukuzumi, S. Catalysis on Electron Transfer and the Mechanistic Insight into Redox Reactions. *Bull. Chem. Soc. Jpn.* **1997**, *70* (1), 1−28.
(164) Fukuzumi, S., Roles of Metal Ions in Controlling Bioinspired Electron-Transfer Systems. Metal Ion-Coupled Electron Transfer. In *Progress in Inorganic Chemistry*; Karlin, K. D., Ed.; John Wiley & Sons Inc: New York, 2009; Vol. *56*, pp 49−153.
(165) Chen, J.; Lee, Y.-M.; Davis, K. M.; Wu, X.; Seo, M. S.; Cho, K.-B.; Yoon, H.; Park, Y. J.; Fukuzumi, S.; Pushkar, Y. N.; Nam, W. A Mononuclear Non-Heme Manganese(IV)−Oxo Complex Binding Redox-Inactive Metal Ions. *J. Am. Chem. Soc.* **2013**, *135* (17), 6388−6391.
(166) Léonard, N. G.; Dhaoui, R.; Chantarojsiri, T.; Yang, J. Y. Electric Fields in Catalysis: From Enzymes to Molecular Catalysts. *ACS Catal.* **2021**, *11* (17), 10923−10932.
(167) Krogman, J. P.; Thomas, C. M. Metal-metal multiple bonding in C_3-symmetric bimetallic complexes of the first row transition metals. *Chem. Commun.* **2014**, *50* (40), 5115−5127.

https://doi.org/10.1021/jacsau.3c00675
JACS Au 2024, 4, 344−368

(168) Cammarota, R. C.; Lu, C. C. Tuning Nickel with Lewis Acidic Group 13 Metalloligands for Catalytic Olefin Hydrogenation. *J. Am. Chem. Soc.* **2015**, *137* (39), 12486−12489.
(169) Lau, T. C.; Mak, C. K. Oxidation of Alkanes by Barium Ruthenate in Acetic-Acid - Catalysis by Lewis-Acids. *J. Chem. Soc. Chem. Comm* **1993**, No. 9, 766−767.
(170) Lau, T. C.; Wu, Z. B.; Bai, Z. L.; Mak, C. K. Lewis-Acid Catalyzed Oxidation of Alkanes by Chromate and Permanganate. *J. Chem. Soc. Dalton* **1995**, No. 4, 695−696.
(171) Xie, N.; Binstead, R. A.; Block, E.; Chandler, W. D.; Lee, D. G.; Meyer, T. J.; Thiruvazhi, M. Reduction of permanganate by thioanisole: Lewis acid catalysis. *J. Org. Chem.* **2000**, *65* (4), 1008−1015.
(172) Lai, S.; Lee, D. G. Lewis acid assisted permanganate oxidations. *Tetrahedron* **2002**, *58* (49), 9879−9887.
(173) Du, H. X.; Lo, P. K.; Hu, Z. M.; Liang, H. J.; Lau, K. C.; Wang, Y. N.; Lam, W. W. Y.; Lau, T. C. Lewis acid-activated oxidation of alcohols by permanganate. *Chem. Commun.* **2011**, *47* (25), 7143−7145.
(174) Ho, C. M.; Lau, T. C. Lewis acid activated oxidation of alkanes by barium ferrate. *New J. Chem.* **2000**, *24* (8), 587−590.
(175) Yiu, S. M.; Wu, Z. B.; Mak, C. K.; Lau, T. C. $FeCl_3$-activated oxidation of alkanes by $[Os(N)O_3]^-$. *J. Am. Chem. Soc.* **2004**, *126* (45), 14921−14929.
(176) Yiu, S. M.; Man, W. L.; Lau, T. C. Efficient catalytic oxidation of alkanes by lewis acid/$[Os^{VI}(N)Cl_4]^-$ using peroxides as terminal oxidants. Evidence for a metal-based active intermediate. *J. Am. Chem. Soc.* **2008**, *130* (32), 10821−10827.
(177) Lam, W. W. Y.; Yiu, S.-M.; Lee, J. M. N.; Yau, S. K. Y.; Kwong, H.-K.; Lau, T.-C.; Liu, D.; Lin, Z. BF_3-Activated Oxidation of Alkanes by MnO_4. *J. Am. Chem. Soc.* **2006**, *128* (9), 2851−2858.
(178) Chen, G.; Ma, L.; Lo, P.-K.; Mak, C.-K.; Lau, K.-C.; Lau, T.-C. Cooperative activating effects of metal ion and Brønsted acid on a metal oxo species. *Chem. Sci.* **2021**, *12* (2), 632−638.
(179) Shi, H.; Cheng, L.; Pan, Y.; Mak, C.-K.; Lau, K.-C.; Lau, T.-C. Synergistic effects of CH_3CO_2H and Ca^{2+} on C−H bond activation by MnO_4^-. *Chem. Sci.* **2022**, *13* (39), 11600−11606.
(180) Dong, L.; Wang, Y. J.; Lv, Y. Z.; Chen, Z. Q.; Mei, F. M.; Xiong, H.; Yin, G. C. Lewis-Acid-Promoted Stoichiometric and Catalytic Oxidations by Manganese Complexes Having Cross-Bridged Cyclam Ligand: A Comprehensive Study. *Inorg. Chem.* **2013**, *52* (9), 5418−5427.
(181) Choe, C.; Yang, L.; Lv, Z.; Mo, W.; Chen, Z.; Li, G.; Yin, G. Redox-inactive metal ions promoted the catalytic reactivity of non-heme manganese complexes towards oxygen atom transfer. *Dalton Trans.* **2015**, *44* (19), 9182−9192.
(182) Chen, Z.; Yang, L.; Choe, C.; Lv, Z.; Yin, G. Non-redox metal ion promoted oxygen transfer by a non-heme manganese catalyst. *Chem. Commun.* **2015**, *51* (10), 1874−1877.
(183) Zhang, Z.; Coats, K. L.; Chen, Z.; Hubin, T. J.; Yin, G. Influence of Calcium(II) and Chloride on the Oxidative Reactivity of a Manganese(II) Complex of a Cross-Bridged Cyclen Ligand. *Inorg. Chem.* **2014**, *53* (22), 11937−11947.
(184) Park, J.; Morimoto, Y.; Lee, Y.-M.; Nam, W.; Fukuzumi, S. Unified View of Oxidative C−H Bond Cleavage and Sulfoxidation by a Nonheme Iron(IV)−Oxo Complex via Lewis Acid-Promoted Electron Transfer. *Inorg. Chem.* **2014**, *53* (7), 3618−3628.
(185) Park, J.; Morimoto, Y.; Lee, Y.-M.; Nam, W.; Fukuzumi, S. Metal Ion Effect on the Switch of Mechanism from Direct Oxygen Transfer to Metal Ion-Coupled Electron Transfer in the Sulfoxidation of Thioanisoles by a Non-Heme Iron(IV)−Oxo Complex. *J. Am. Chem. Soc.* **2011**, *133* (14), 5236−5239.
(186) Park, J.; Morimoto, Y.; Lee, Y.-M.; Nam, W.; Fukuzumi, S. Proton-Promoted Oxygen Atom Transfer vs Proton-Coupled Electron Transfer of a Non-Heme Iron(IV)-Oxo Complex. *J. Am. Chem. Soc.* **2012**, *134* (8), 3903−3911.
(187) Mandimutsira, B. S.; Ramdhanie, B.; Todd, R. C.; Wang, H.; Zareba, A. A.; Czernuszewicz, R. S.; Goldberg, D. P. A Stable Manganese(V)-Oxo Corrolazine Complex. *J. Am. Chem. Soc.* **2002**, *124* (51), 15170−15171.
(188) Neu, H. M.; Yang, T.; Baglia, R. A.; Yosca, T. H.; Green, M. T.; Quesne, M. G.; de Visser, S. P.; Goldberg, D. P. Oxygen-Atom Transfer Reactivity of Axially Ligated Mn(V)−Oxo Complexes: Evidence for Enhanced Electrophilic and Nucleophilic Pathways. *J. Am. Chem. Soc.* **2014**, *136* (39), 13845−13852.
(189) Prokop, K. A.; Neu, H. M.; de Visser, S. P.; Goldberg, D. P. A Manganese(V)−Oxo π-Cation Radical Complex: Influence of One-Electron Oxidation on Oxygen-Atom Transfer. *J. Am. Chem. Soc.* **2011**, *133* (40), 15874−15877.
(190) Zaragoza, J. P. T.; Baglia, R. A.; Siegler, M. A.; Goldberg, D. P. Strong Inhibition of O-Atom Transfer Reactivity for $Mn^{IV}(O)$(π-Radical-Cation)(Lewis Acid) versus $Mn^{V}(O)$ Porphyrinoid Complexes. *J. Am. Chem. Soc.* **2015**, *137* (20), 6531−6540.
(191) Bullock, J. P.; Bond, A. M.; Boeré, R. T.; Gietz, T. M.; Roemmele, T. L.; Seagrave, S. D.; Masuda, J. D.; Parvez, M. Synthesis, Characterization, and Electrochemical Studies of $PPh_{3-n}(dipp)_n$ (dipp = 2,6-Diisopropylphenyl): Steric and Electronic Effects on the Chemical and Electrochemical Oxidation of a Homologous Series of Triarylphosphines and the Reactivities of the Corresponding Phosphoniumyl Radical Cations. *J. Am. Chem. Soc.* **2013**, *135* (30), 11205−11215.
(192) Yang, T.; Quesne, M. G.; Neu, H. M.; Cantú Reinhard, F. G.; Goldberg, D. P.; de Visser, S. P. Singlet versus Triplet Reactivity in an Mn(V)−Oxo Species: Testing Theoretical Predictions Against Experimental Evidence. *J. Am. Chem. Soc.* **2016**, *138* (38), 12375−12386.
(193) Zhu, C.; Liang, J.; Wang, B.; Zhu, J.; Cao, Z. Significant effect of spin flip on the oxygen atom transfer reaction from (oxo)-manganese(v) corroles to thioanisole: insights from density functional calculations. *Phys. Chem. Chem. Phys.* **2012**, *14* (37), 12800−12806.
(194) Miller, C. G.; Gordon-Wylie, S. W.; Horwitz, C. P.; Strazisar, S. A.; Peraino, D. K.; Clark, G. R.; Weintraub, S. T.; Collins, T. J. A Method for Driving O-Atom Transfer: Secondary Ion Binding to a Tetraamide Macrocyclic Ligand. *J. Am. Chem. Soc.* **1998**, *120* (44), 11540−11541.
(195) Popescu, D.-L.; Chanda, A.; Stadler, M.; de Oliveira, F. T.; Ryabov, A. D.; Münck, E.; Bominaar, E. L.; Collins, T. J. High-valent first-row transition-metal complexes of tetraamido (4N) and diamidodialkoxido or diamidophenolato (2N/2O) ligands: Synthesis, structure, and magnetochemistry. *Coord. Chem. Rev.* **2008**, *252* (18−20), 2050−2071.
(196) Que, L.; Ho, R. Y. N. Dioxygen Activation by Enzymes with Mononuclear Non-Heme Iron Active Sites. *Chem. Rev.* **1996**, *96* (7), 2607−2624.
(197) Wallar, B. J.; Lipscomb, J. D. Dioxygen Activation by Enzymes Containing Binuclear Non-Heme Iron Clusters. *Chem. Rev.* **1996**, *96* (7), 2625−2658.
(198) Merkx, M.; Kopp, D. A.; Sazinsky, M. H.; Blazyk, J. L.; Müller, J.; Lippard, S. J. Dioxygen Activation and Methane Hydroxylation by Soluble Methane Monooxygenase: A Tale of Two Irons and Three Proteins. *Angew. Chem., Int. Ed.* **2001**, *40* (15), 2782−2807.
(199) Decker, A.; Solomon, E. I. Dioxygen activation by copper, heme and non-heme iron enzymes: comparison of electronic structures and reactivities. *Curr. Opin. Chem. Biol.* **2005**, *9* (2), 152−163.
(200) Denisov, I. G.; Makris, T. M.; Sligar, S. G.; Schlichting, I. Structure and Chemistry of Cytochrome P450. *Chem. Rev.* **2005**, *105* (6), 2253−2278.
(201) Kal, S.; Que, L. Dioxygen activation by nonheme iron enzymes with the 2-His-1-carboxylate facial triad that generate high-valent oxoiron oxidants. *JBIC Journal of Biological Inorganic Chemistry* **2017**, *22* (2), 339−365.
(202) Lemon, C. M.; Dogutan, D. K.; Nocera, D. G. In *Porphyrin and corrole platforms for water oxidation, oxygen reduction, and peroxide dismutation*; World Scientific Publishing Co. Pte. Ltd., 2012; pp 1−143.

https://doi.org/10.1021/jacsau.3c00675
JACS Au 2024, 4, 344−368

(203) Weiss, R.; Gold, A.; Trautwein, A. X.; Terner, J. In *High-valent iron and manganese complexes of porphyrins and related macrocycles*; Academic Press: 2000; pp 65−96.
(204) Cho, J.; Sarangi, R.; Nam, W. Mononuclear Metal−O_2 Complexes Bearing Macrocyclic N-Tetramethylated Cyclam Ligands. *Acc. Chem. Res.* **2012**, *45* (8), 1321−1330.
(205) Chufán, E. E.; Puiu, S. C.; Karlin, K. D. Heme−Copper/Dioxygen Adduct Formation, Properties, and Reactivity. *Acc. Chem. Res.* **2007**, *40* (7), 563−572.
(206) Cook, S. A.; Borovik, A. S. Molecular Designs for Controlling the Local Environments around Metal Ions. *Acc. Chem. Res.* **2015**, *48* (8), 2407−2414.
(207) Kieber-Emmons, M. T.; Riordan, C. G. Dioxygen Activation at Monovalent Nickel. *Acc. Chem. Res.* **2007**, *40* (7), 618−625.
(208) Korendovych, I. V.; Kryatov, S. V.; Rybak-Akimova, E. V. Dioxygen Activation at Non-Heme Iron: Insights from Rapid Kinetic Studies. *Acc. Chem. Res.* **2007**, *40* (7), 510−521.
(209) Rosenthal, J.; Nocera, D. G. Role of Proton-Coupled Electron Transfer in O−O Bond Activation. *Acc. Chem. Res.* **2007**, *40* (7), 543−553.
(210) Suzuki, M. Ligand Effects on Dioxygen Activation by Copper and Nickel Complexes: Reactivity and Intermediates. *Acc. Chem. Res.* **2007**, *40* (7), 609−617.
(211) Yao, S.; Driess, M. Lessons from Isolable Nickel(I) Precursor Complexes for Small Molecule Activation. *Acc. Chem. Res.* **2012**, *45* (2), 276−287.
(212) Klotz, I. M.; Kurtz, D. M. Metal-Dioxygen Complexes: A Perspective. *Chem. Rev.* **1994**, *94* (3), 567−568.
(213) Lewis, E. A.; Tolman, W. B. Reactivity of Dioxygen−Copper Systems. *Chem. Rev.* **2004**, *104* (2), 1047−1076.
(214) Mirica, L. M.; Ottenwaelder, X.; Stack, T. D. P. Structure and Spectroscopy of Copper−Dioxygen Complexes. *Chem. Rev.* **2004**, *104* (2), 1013−1046.
(215) Zhang, W.; Lai, W.; Cao, R. Energy-Related Small Molecule Activation Reactions: Oxygen Reduction and Hydrogen and Oxygen Evolution Reactions Catalyzed by Porphyrin- and Corrole-Based Systems. *Chem. Rev.* **2017**, *117* (4), 3717−3797.
(216) Fukuzumi, S.; Karlin, K. D. Kinetics and thermodynamics of formation and electron-transfer reactions of Cu−O2 and Cu2−O2 complexes. *Coord. Chem. Rev.* **2013**, *257* (1), 187−195.
(217) Hong, S.; Lee, Y.-M.; Ray, K.; Nam, W. Dioxygen activation chemistry by synthetic mononuclear nonheme iron, copper and chromium complexes. *Coord. Chem. Rev.* **2017**, *334*, 25−42.
(218) Liang, H.-C.; Dahan, M.; Karlin, K. D. Dioxygen-activating bio-inorganic model complexes. *Curr. Opin. Chem. Biol.* **1999**, *3* (2), 168−175.
(219) Engelmann, X.; Monte-Pérez, I.; Ray, K. Oxidation Reactions with Bioinspired Mononuclear Non-Heme Metal−Oxo Complexes. *Angew. Chem., Int. Ed.* **2016**, *55* (27), 7632−7649.
(220) Rosenthal, J.; Nocera, D. G. Oxygen Activation Chemistry of Pacman and Hangman Porphyrin Architectures Based on Xanthene and Dibenzofuran Spacers. In *Progress in Inorganic Chemistry*; John Wiley & Sons, Inc.: 2008; pp 483−544.
(221) Fukuzumi, S.; Ohtsu, H.; Ohkubo, K.; Itoh, S.; Imahori, H. Formation of superoxide−metal ion complexes and the electron transfer catalysis. *Coord. Chem. Rev.* **2002**, *226* (1−2), 71−80.
(222) Fukuzumi, S.; Patz, M.; Suenobu, T.; Kuwahara, Y.; Itoh, S. ESR Spectra of Superoxide Anion−Scandium Complexes Detectable in Fluid Solution. *J. Am. Chem. Soc.* **1999**, *121* (7), 1605−1606.
(223) Ohkubo, K.; Menon, S. C.; Orita, A.; Otera, J.; Fukuzumi, S. Quantitative Evaluation of Lewis Acidity of Metal Ions with Different Ligands and Counterions in Relation to the Promoting Effects of Lewis Acids on Electron Transfer Reduction of Oxygen. *Journal of Organic Chemistry* **2003**, *68* (12), 4720−4726.
(224) Sawyer, D. T.; Calderwood, T. S.; Yamaguchi, K.; Angelis, C. T. Synthesis and characterization of tetramethylammonium superoxide. *Inorg. Chem.* **1983**, *22* (18), 2577−2583.
(225) Fukuzumi, S. Metal Ion-coupled Electron-transfer Reduction of Dioxygen. *Chem. Lett.* **2008**, *37* (8), 808−813.
(226) Fukuzumi, S.; Ohkubo, K. Fluorescence Maxima of 10-Methylacridone−Metal Ion Salt Complexes: A Convenient and Quantitative Measure of Lewis Acidity of Metal Ion Salts. *J. Am. Chem. Soc.* **2002**, *124* (35), 10270−10271.
(227) Lee, Y.-M.; Bang, S.; Kim, Y. M.; Cho, J.; Hong, S.; Nomura, T.; Ogura, T.; Troeppner, O.; Ivanovic-Burmazovic, I.; Sarangi, R.; Fukuzumi, S.; Nam, W. A mononuclear nonheme iron(III)-peroxo complex binding redox-inactive metal ions. *Chem. Sci.* **2013**, *4* (10), 3917−3923.
(228) Bang, S.; Lee, Y.-M.; Hong, S.; Cho, K.-B.; Nishida, Y.; Seo, M. S.; Sarangi, R.; Fukuzumi, S.; Nam, W. Redox-inactive metal ions modulate the reactivity and oxygen release of mononuclear non-haem iron(III)−peroxo complexes. *Nat. Chem.* **2014**, *6* (10), 934−940.
(229) Bae, S. H.; Lee, Y.-M.; Fukuzumi, S.; Nam, W. Fine Control of the Redox Reactivity of a Nonheme Iron(III)−Peroxo Complex by Binding Redox-Inactive Metal Ions. *Angew. Chem., Int. Ed.* **2017**, *56* (3), 801−805.
(230) Karmalkar, D. G.; Seo, M. S.; Lee, Y.-M.; Kim, Y.; Lee, E.; Sarangi, R.; Fukuzumi, S.; Nam, W. Deeper Understanding of Mononuclear Manganese(IV)−Oxo Binding Brønsted and Lewis Acids and the Manganese(IV)−Hydroxide Complex. *Inorg. Chem.* **2021**, *60* (22), 16996−17007.
(231) Dalle, K. E.; Gruene, T.; Dechert, S.; Demeshko, S.; Meyer, F. Weakly Coupled Biologically Relevant $Cu^{II2}(\mu\text{-}\eta^1\text{:}\eta^1\text{-}O_2)$ cis-Peroxo Adduct that Binds Side-On to Additional Metal Ions. *J. Am. Chem. Soc.* **2014**, *136* (20), 7428−7434.
(232) Duerr, K.; Olah, J.; Davydov, R.; Kleimann, M.; Li, J.; Lang, N.; Puchta, R.; Hubner, E.; Drewello, T.; Harvey, J. N.; Jux, N.; Ivanovic-Burmazovic, I. Studies on an iron(III)-peroxo porphyrin. Iron(III)-peroxo or iron(II)-superoxo? *Dalton Trans.* **2010**, *39* (8), 2049−2056.
(233) Dürr, K.; Macpherson, B. P.; Warratz, R.; Hampel, F.; Tuczek, F.; Helmreich, M.; Jux, N.; Ivanović-Burmazović, I. Iron(III) Complex of a Crown Ether−Porphyrin Conjugate and Reversible Binding of Superoxide to Its Iron(II) Form. *J. Am. Chem. Soc.* **2007**, *129* (14), 4217−4228.
(234) Schax, F.; Suhr, S.; Bill, E.; Braun, B.; Herwig, C.; Limberg, C. A Heterobimetallic Superoxide Complex formed through O_2 Activation between Chromium(II) and a Lithium Cation. *Angew. Chem., Int. Ed.* **2015**, *54* (4), 1352−1356.
(235) Lee, Y.-M.; Bang, S.; Yoon, H.; Bae, S. H.; Hong, S.; Cho, K.-B.; Sarangi, R.; Fukuzumi, S.; Nam, W. Tuning the Redox Properties of a Nonheme Iron(III)−Peroxo Complex Binding Redox-Inactive Zinc Ions by Water Molecules. *Chem.—Eur. J.* **2015**, *21* (30), 10676−10680.
(236) Li, F.; Van Heuvelen, K. M.; Meier, K. K.; Münck, E.; Que, L. Sc^{3+}-Triggered Oxoiron(IV) Formation from O_2 and its Non-Heme Iron(II) Precursor via a Sc^{3+}−Peroxo−Fe^{3+} Intermediate. *J. Am. Chem. Soc.* **2013**, *135* (28), 10198−10201.
(237) Thibon, A.; England, J.; Martinho, M.; Young, V. G.; Frisch, J. R.; Guillot, R.; Girerd, J.-J.; Münck, E.; Que, L.; Banse, F. Proton- and Reductant-Assisted Dioxygen Activation by a Nonheme Iron(II) Complex to Form an Oxoiron(IV) Intermediate. *Angew. Chem., Int. Ed.* **2008**, *47* (37), 7064−7067.
(238) Wallen, C. M.; Wielizcko, M.; Bacsa, J.; Scarborough, C. C. Heterotrimetallic sandwich complexes supported by sulfonamido ligands. *Inorganic Chemistry Frontiers* **2016**, *3* (1), 142−149.
(239) Kim, K.; Cho, D.; Noh, H.; Ohta, T.; Baik, M.-H.; Cho, J. Controlled Regulation of the Nitrile Activation of a Peroxocobalt(III) Complex with Redox-Inactive Lewis Acidic Metals. *J. Am. Chem. Soc.* **2021**, *143* (30), 11382−11392.
(240) Kim, B.; Kim, S.; Ohta, T.; Cho, J. Redox-Inactive Metal Ions That Enhance the Nucleophilic Reactivity of an Alkylperoxocopper-(II) Complex. *Inorg. Chem.* **2020**, *59* (14), 9938−9943.
(241) Kal, S.; Draksharapu, A.; Que, L. Sc^{3+} (or $HClO_4$) Activation of a Nonheme Fe^{III}−OOH Intermediate for the Rapid Hydroxylation of Cyclohexane and Benzene. *J. Am. Chem. Soc.* **2018**, *140* (17), 5798−5804.

https://doi.org/10.1021/jacsau.3c00675
JACS Au 2024, 4, 344−368

(242) Que, J. L., Jr.; Tolman, W. B. Bis(μ-oxo)dimetal "Diamond" Cores in Copper and Iron Complexes Relevant to Biocatalysis. *Angew. Chem., Int. Ed.* **2002**, *41* (11), 1821−1821.
(243) Aboelella, N. W.; York, J. T.; Reynolds, A. M.; Fujita, K.; Kinsinger, C. R.; Cramer, C. J.; Riordan, C. G.; Tolman, W. B. Mixed metal bis(μ-oxo) complexes with $[CuM(\mu\text{-}O)_2]^{n+}$ (M = Ni(III) or Pd(II)) cores. *Chem. Commun.* **2004**, No. 15, 1716−1717.
(244) York, J. T.; Llobet, A.; Cramer, C. J.; Tolman, W. B. Heterobimetallic Dioxygen Activation: Synthesis and Reactivity of Mixed Cu−Pd and Cu−Pt Bis(μ-oxo) Complexes. *J. Am. Chem. Soc.* **2007**, *129* (25), 7990−7999.
(245) Yao, S.; Xiong, Y.; Vogt, M.; Grützmacher, H.; Herwig, C.; Limberg, C.; Driess, M. O-O Bond Activation in Heterobimetallic Peroxides: Synthesis of the Peroxide $[LNi(\mu,\eta^2{:}\eta^2\text{-}O_2)K]$ and its Conversion into a Bis(μ-Hydroxo) Nickel Zinc Complex. *Angew. Chem., Int. Ed.* **2009**, *48* (43), 8107−8110.
(246) Yao, S.; Herwig, C.; Xiong, Y.; Company, A.; Bill, E.; Limberg, C.; Driess, M. Monooxygenase-Like Reactivity of an Unprecedented Heterobimetallic $\{FeO_2Ni\}$ Moiety. *Angew. Chem., Int. Ed.* **2010**, *49* (39), 7054−7058.
(247) Kundu, S.; Pfaff, F. F.; Miceli, E.; Zaharieva, I.; Herwig, C.; Yao, S.; Farquhar, E. R.; Kuhlmann, U.; Bill, E.; Hildebrandt, P.; Dau, H.; Driess, M.; Limberg, C.; Ray, K. A High-Valent Heterobimetallic $[Cu^{III}(\mu\text{-}O)_2Ni^{III}]^{2+}$ Core with Nucleophilic Oxo Groups. *Angew. Chem., Int. Ed.* **2013**, *52* (21), 5622−5626.
(248) Engelmann, X.; Yao, S.; Farquhar, E. R.; Szilvási, T.; Kuhlmann, U.; Hildebrandt, P.; Driess, M.; Ray, K. A New Domain of Reactivity for High-Valent Dinuclear $[M(\mu\text{-}O)_2M']$ Complexes in Oxidation Reactions. *Angew. Chem., Int. Ed.* **2017**, *56* (1), 297−301.
(249) Garcia-Bosch, I.; Cowley, R. E.; Díaz, D. E.; Peterson, R. L.; Solomon, E. I.; Karlin, K. D. Substrate and Lewis Acid Coordination Promote O−O Bond Cleavage of an Unreactive $L_2Cu^{II2}(O_2^{2-})$ Species to Form $L_2Cu^{III2}(O)_2$ Cores with Enhanced Oxidative Reactivity. *J. Am. Chem. Soc.* **2017**, *139* (8), 3186−3195.
(250) Park, G. Y.; Qayyum, M. F.; Woertink, J.; Hodgson, K. O.; Hedman, B.; Narducci Sarjeant, A. A.; Solomon, E. I.; Karlin, K. D. Geometric and Electronic Structure of $[\{Cu(MeAN)\}_2(\mu\text{-}\eta^2{:}\eta^2(O_2^{2-}))]^{2+}$ with an Unusually Long O−O Bond: O−O Bond Weakening vs Activation for Reductive Cleavage. *J. Am. Chem. Soc.* **2012**, *134* (20), 8513−8524.
(251) Kakuda, S.; Rolle, C. J.; Ohkubo, K.; Siegler, M. A.; Karlin, K. D.; Fukuzumi, S. Lewis Acid-Induced Change from Four- to Two-Electron Reduction of Dioxygen Catalyzed by Copper Complexes Using Scandium Triflate. *J. Am. Chem. Soc.* **2015**, *137* (9), 3330−3337.
(252) Fukuzumi, S.; Kotani, H.; Lucas, H. R.; Doi, K.; Suenobu, T.; Peterson, R. L.; Karlin, K. D. Mononuclear Copper Complex-Catalyzed Four-Electron Reduction of Oxygen. *J. Am. Chem. Soc.* **2010**, *132* (20), 6874−6875.
(253) Guilard, R.; Brandes, S.; Tardieux, C.; Tabard, A.; L'Her, M.; Miry, C.; Gouerec, P.; Knop, Y.; Collman, J. P. Synthesis and Characterization of Cofacial Metallodiporphyrins Involving Cobalt and Lewis Acid Metals: New Dinuclear Multielectron Redox Catalysts of Dioxygen Reduction. *J. Am. Chem. Soc.* **1995**, *117* (47), 11721−11729.
(254) Collman, J. P.; Hendricks, N. H.; Kim, K.; Bencosme, C. S. The role of Lewis acids in promoting the electrocatalytic four-electron reduction of dioxygen. *J. Chem. Soc., Chem. Commun.* **1987**, No. 20, 1537−1538.
(255) Collman, J. P.; Denisevich, P.; Konai, Y.; Marrocco, M.; Koval, C.; Anson, F. C. Electrode Catalysis of the 4-Electron Reduction of Oxygen to Water by Dicobalt Face-to-Face Porphyrins. *J. Am. Chem. Soc.* **1980**, *102* (19), 6027−6036.
(256) Yachandra, V. K.; Yano, J. Calcium in the oxygen-evolving complex: Structural and mechanistic role determined by X-ray spectroscopy. *Journal of Photochemistry and Photobiology B: Biology* **2011**, *104* (1−2), 51−59.
(257) Lee, C.-I.; Brudvig, G. W. Investigation of the Functional Role of Ca^{2+} in the Oxygen-Evolving Complex of Photosystem II: A pH-Dependence Study of the Substitution of Ca^{2+} by Sr^{2+}. *Journal of the Chinese Chemical Society* **2004**, *51* (5B), 1221−1228.
(258) Vrettos, J. S.; Stone, D. A.; Brudvig, G. W. Quantifying the Ion Selectivity of the Ca^{2+} Site in Photosystem II: Evidence for Direct Involvement of Ca^{2+} in O_2 Formation. *Biochemistry* **2001**, *40* (26), 7937−7945.
(259) Young, I. D.; Ibrahim, M.; Chatterjee, R.; Gul, S.; Fuller, F. D.; Koroidov, S.; Brewster, A. S.; Tran, R.; Alonso-Mori, R.; Kroll, T.; Michels-Clark, T.; Laksmono, H.; Sierra, R. G.; Stan, C. A.; Hussein, R.; Zhang, M.; Douthit, L.; Kubin, M.; de Lichtenberg, C.; Vo Pham, L.; Nilsson, H.; Cheah, M. H.; Shevela, D.; Saracini, C.; Bean, M. A.; Seuffert, I.; Sokaras, D.; Weng, T.-C.; Pastor, E.; Weninger, C.; Fransson, T.; Lassalle, L.; Bräuer, P.; Aller, P.; Docker, P. T.; Andi, B.; Orville, A. M.; Glownia, J. M.; Nelson, S.; Sikorski, M.; Zhu, D.; Hunter, M. S.; Lane, T. J.; Aquila, A.; Koglin, J. E.; Robinson, J.; Liang, M.; Boutet, S.; Lyubimov, A. Y.; Uervirojnangkoorn, M.; Moriarty, N. W.; Liebschner, D.; Afonine, P. V.; Waterman, D. G.; Evans, G.; Wernet, P.; Dobbek, H.; Weis, W. I.; Brunger, A. T.; Zwart, P. H.; Adams, P. D.; Zouni, A.; Messinger, J.; Bergmann, U.; Sauter, N. K.; Kern, J.; Yachandra, V. K.; Yano, J. Structure of Photosystem II and Substrate Binding at Room Temperature. *Nature* **2016**, *540* (7633), 453−457.
(260) Suga, M.; Akita, F.; Hirata, K.; Ueno, G.; Murakami, H.; Nakajima, Y.; Shimizu, T.; Yamashita, K.; Yamamoto, M.; Ago, H.; Shen, J.-R. Native Structure of Photosystem II at 1.95 Å Resolution Viewed by Femtosecond X-ray Pulses. *Nature* **2015**, *517* (7532), 99−103.
(261) Umena, Y.; Kawakami, K.; Shen, J.-R.; Kamiya, N. Crystal Structure of Oxygen-Evolving Photosystem II at a Resolution of 1.9 Å. *Nature* **2011**, *473* (7345), 55−60.
(262) Ferreira, K. N.; Iverson, T. M.; Maghlaoui, K.; Barber, J.; Iwata, S. Architecture of the Photosynthetic Oxygen-Evolving Center. *Science* **2004**, *303* (5665), 1831−1838.
(263) Yano, J.; Yachandra, V. Mn_4Ca Cluster in Photosynthesis: Where and How Water is Oxidized to Dioxygen. *Chem. Rev.* **2014**, *114* (8), 4175−4205.
(264) Hunter, B. M.; Gray, H. B.; Müller, A. M. Earth-Abundant Heterogeneous Water Oxidation Catalysts. *Chem. Rev.* **2016**, *116* (22), 14120−14136.
(265) Kanan, M. W.; Nocera, D. G. In Situ Formation of an Oxygen-Evolving Catalyst in Neutral Water Containing Phosphate and Co^{2+}. *Science* **2008**, *321* (5892), 1072−1075.
(266) Risch, M.; Khare, V.; Zaharieva, I.; Gerencser, L.; Chernev, P.; Dau, H. Cobalt−Oxo Core of a Water-Oxidizing Catalyst Film. *J. Am. Chem. Soc.* **2009**, *131* (20), 6936−6937.
(267) Kanan, M. W.; Yano, J.; Surendranath, Y.; Dincă, M.; Yachandra, V. K.; Nocera, D. G. Structure and Valency of a Cobalt−Phosphate Water Oxidation Catalyst Determined by in Situ X-ray Spectroscopy. *J. Am. Chem. Soc.* **2010**, *132* (39), 13692−13701.
(268) Yamada, Y.; Oyama, K.; Suenobu, T.; Fukuzumi, S. Photocatalytic water oxidation by persulphate with a Ca^{2+} ion-incorporated polymeric cobalt cyanide complex affording O_2 with 200% quantum efficiency. *Chem. Commun.* **2017**, *53* (24), 3418−3421.
(269) Lucht, K. P.; Mendoza-Cortes, J. L. Birnessite: A Layered Manganese Oxide To Capture Sunlight for Water-Splitting Catalysis. *J. Phys. Chem. C* **2015**, *119* (40), 22838−22846.
(270) Chen, J. Y. C.; Miller, J. T.; Gerken, J. B.; Stahl, S. S. Inverse spinel $NiFeAlO_4$ as a highly active oxygen evolution electrocatalyst: promotion of activity by a redox-inert metal ion. *Energy Environ. Sci.* **2014**, *7* (4), 1382−1386.
(271) Gerken, J. B.; Shaner, S. E.; Masse, R. C.; Porubsky, N. J.; Stahl, S. S. A survey of diverse earth abundant oxygen evolution electrocatalysts showing enhanced activity from Ni-Fe oxides containing a third metal. *Energy Environ. Sci.* **2014**, *7* (7), 2376−2382.
(272) Sarma, R.; Angeles-Boza, A. M.; Brinkley, D. W.; Roth, J. P. Studies of the Di-iron(VI) Intermediate in Ferrate-Dependent Oxygen Evolution from Water. *J. Am. Chem. Soc.* **2012**, *134* (37), 15371−15386.

https://doi.org/10.1021/jacsau.3c00675
JACS Au 2024, 4, 344−368

(273) Goff, H.; Murmann, R. K. Mechanism of isotopic oxygen exchange and reduction of ferrate(VI) ion (FeO_4^{2-}). *J. Am. Chem. Soc.* **1971**, *93* (23), 6058−6065.
(274) Ma, L.; Lam, W. W. Y.; Lo, P.-K.; Lau, K.-C.; Lau, T.-C. Ca^{2+}-Induced Oxygen Generation by FeO_4^{2-} at pH 9−10. *Angew. Chem., Int. Ed.* **2016**, *55* (9), 3012−3016.
(275) Rice, D. B.; Grotemeyer, E. N.; Donovan, A. M.; Jackson, T. A. Effect of Lewis Acids on the Structure and Reactivity of a Mononuclear Hydroxomanganese(III) Complex. *Inorg. Chem.* **2020**, *59* (5), 2689−2700.
(276) Morimoto, Y.; Park, J.; Suenobu, T.; Lee, Y.-M.; Nam, W.; Fukuzumi, S. Mechanistic Borderline of One-Step Hydrogen Atom Transfer versus Stepwise Sc^{3+}-Coupled Electron Transfer from Benzyl Alcohol Derivatives to a Non-Heme Iron(IV)-Oxo Complex. *Inorg. Chem.* **2012**, *51* (18), 10025−10036.
(277) Baglia, R. A.; Krest, C. M.; Yang, T.; Leeladee, P.; Goldberg, D. P. High-Valent Manganese−Oxo Valence Tautomers and the Influence of Lewis/Brönsted Acids on C−H Bond Cleavage. *Inorg. Chem.* **2016**, *55* (20), 10800−10809.
(278) Zhang, J.; Yang, H.; Sun, T.; Chen, Z.; Yin, G. Nonredox Metal-Ions-Enhanced Dioxygen Activation by Oxidovanadium(IV) Complexes toward Hydrogen Atom Abstraction. *Inorg. Chem.* **2017**, *56* (2), 834−844.
(279) Léonard, N. G.; Chantarojsiri, T.; Ziller, J. W.; Yang, J. Y. Cationic Effects on the Net Hydrogen Atom Bond Dissociation Free Energy of High-Valent Manganese Imido Complexes. *J. Am. Chem. Soc.* **2022**, *144* (4), 1503−1508.
(280) Bordwell, F. G. Equilibrium acidities in dimethyl sulfoxide solution. *Acc. Chem. Res.* **1988**, *21* (12), 456−463.
(281) Reed, C. J.; Agapie, T. Thermodynamics of Proton and Electron Transfer in Tetranuclear Clusters with Mn−OH_2/OH Motifs Relevant to H_2O Activation by the Oxygen Evolving Complex in Photosystem II. *J. Am. Chem. Soc.* **2018**, *140* (34), 10900−10908.
(282) Reed, C. J.; Agapie, T. A terminal Fe^{III}−Oxo in a Tetranuclear Cluster: Effects of Distal Metal Centers on Structure and Reactivity. *J. Am. Chem. Soc.* **2019**, *141* (24), 9479−9484.

https://doi.org/10.1021/jacsau.3c00675
JACS Au 2024, 4, 344−368